NASA/TM—2015–218812

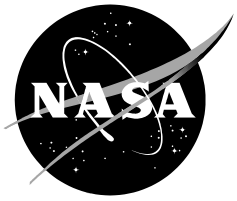

Full-Scale Prop-Rotor Stability Tests on the XV3 at High Advance Ratios

David G. Koenig
Ames Research Center
Moffett Field, California

Joseph P. Morelli
U.U.S. Army Aeronautical Research Laboratory
Ames Research Center
Moffett Field, California

May 2015

NASA STI Program ... in Profile

Since its founding, NASA has been dedicated to the advancement of aeronautics and space science. The NASA scientific and technical information (STI) program plays a key part in helping NASA maintain this important role.

The NASA STI program operates under the auspices of the Agency Chief Information Officer. It collects, organizes, provides for archiving, and disseminates NASA's STI. The NASA STI program provides access to the NTRS Registered and its public interface, the NASA Technical Reports Server, thus providing one of the largest collections of aeronautical and space science STI in the world. Results are published in both non-NASA channels and by NASA in the NASA STI Report Series, which includes the following report types:

- TECHNICAL PUBLICATION. Reports of completed research or a major significant phase of research that present the results of NASA Programs and include extensive data or theoretical analysis. Includes compilations of significant scientific and technical data and information deemed to be of continuing reference value. NASA counterpart of peer-reviewed formal professional papers but has less stringent limitations on manuscript length and extent of graphic presentations.

- TECHNICAL MEMORANDUM. Scientific and technical findings that are preliminary or of specialized interest, e.g., quick release reports, working papers, and bibliographies that contain minimal annotation. Does not contain extensive analysis.

- CONTRACTOR REPORT. Scientific and technical findings by NASA-sponsored contractors and grantees.

- CONFERENCE PUBLICATION. Collected papers from scientific and technical conferences, symposia, seminars, or other meetings sponsored or co-sponsored by NASA.

- SPECIAL PUBLICATION. Scientific, technical, or historical information from NASA programs, projects, and missions, often concerned with subjects having substantial public interest.

- TECHNICAL TRANSLATION. English-language translations of foreign scientific and technical material pertinent to NASA's mission.

Specialized services also include organizing and publishing research results, distributing specialized research announcements and feeds, providing information desk and personal search support, and enabling data exchange services.

For more information about the NASA STI program, see the following:

- Access the NASA STI program home page at http://www.sti.nasa.gov

- E-mail your question to help@sti.nasa.gov

- Phone the NASA STI Information Desk at 757-864-9658

- Write to:
  NASA STI Information Desk
  Mail Stop 148
  NASA Langley Research Center
  Hampton, VA 23681-2199

NASA/TM—2015–218812

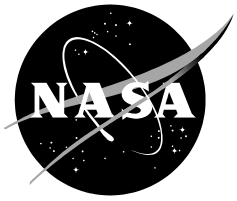

Full-Scale Prop-Rotor Stability Tests on the XV3 at High Advance Ratios

David G. Koenig
Ames Research Center
Moffett Field, California

Joseph P. Morelli
U.U.S. Army Aeronautical Research Laboratory
Ames Research Center
Moffett Field, California

National Aeronautics and
Space Administration

Ames Research Center
Moffett Field, CA 94035-1000

May 2015

Available from:

NASA Center for AeroSpace Information
7115 Standard Drive
Hanover, MD 21076-1320
443-757-5802

National Technical Information Service
5301 Shawnee Road
Alexandria, VA 22312
703-605-6000

This report is also available in electronic form at

http:/ntrs.nasa.gov

TABLE OF CONTENTS

LIST OF FIGURES

LIST OF TABLES

SUMMARY

Tests in the 40- by 80-foot wind tunnel were made at airspeeds from 40 to 195 knots. The aircraft was mounted with and without roll freedom. Rotor pylon configuration variables included the following: swashplate stabilization by mechanically coupling the swashplate to the wing or fuselage; pylon restraint stiffness and damping; hub restraint; and delta-three combined with swashplate retardation. Time histories were recorded of pylon motions and rotor loads following pulse-type excitations of the pylon. It was found that damping of the low frequency whirl mode increased with swashplate stabilization, pylon stiffness, and hub restraint.

INTRODUCTION

The results of wind tunnel and flight tests on the XV-3 are presented in references 1, 2, and 3. During the flight tests, the aircraft was converted between helicopter and airplane mode with no difficulty. At high prop-rotor advance ratios, large flapping angles coupled with precession of the rotor produced in-plane forces which tended to reduce the short period damping of the aircraft. Delta-three (pitch-flap coupling) and flapping hinge restraint were proposed as possible solutions.

Preliminary to further flight testing, full-scale wind tunnel tests were made in 1962. During these tests a pylon-rotor instability was experienced at 130 knots with a delta-three of 20°. Control modifications combined with flapping hinge restraint increased the speed limit to

160 knots, but it was found that delta-three adversely affected rotor stability. The instability was characterized by a low frequency precession of the pylon-rotor system in a direction opposite to rotor rotation (backward whirl mode).

An analytical and experimental program was initiated by the Bell Helicopter Company which resulted in the definition of and study of several modes of pylon-rotor instability. Results of this program are presented in reference 4 where it is shown that the mode of instability encountered in the 1962 tests, namely, a backward rotor whirl mode, could be predicted both by computer and by small scale model test results and had a frequency of about .1 to .3 per rev. This is in contrast to the forward pylon whirl mode which has a frequency near that of the pylon support natural frequency. For either of the whirl modes, in-plane forces due to flapping are phased in a direction that contributes to the instability at high advance ratios. Analyses and results of small scale tests indicated that these forces could be reduced or eliminated by modifications to the rotor control system. With one of these modifications, the swashplate (and hence the rotor tip path plane) is coupled to the wing tip or fuselage rather than to the pylon in order to maintain a favorable orientation of the tip path plane with respect to the aircraft. Another modification, swashplate retardation (a re-indexing of the swashplate with respect to the blades), was found to minimize the adverse effects of delta-three.

A full-scale wind tunnel program was initiated to verify the theoretical analysis as well as to investigate rotor-pylon configurations designed to improve pylon-rotor stability. Configurations investigated

were flapping hinge restraint, pylon mount stiffness, and swashplate coupling to either the pylon, wing, or fuselage. These configurations were tested for nominal values of delta-three of 22 and 35°. Tests were made on both the conventional wind tunnel support with attachment points at the wing and with a mount which allowed the aircraft to roll. The latter mount or roll free mount was considered as a result of computer studies which showed that wing tip vertical or roll freedom would adversely affect measured rotor stability levels.

NOTATION

K_b	hub spring stiffness per blade, in-lb/blade
k_x and k_y	swashplate coupling in pitch and yaw respectively; will be 0 if swashplate is pylon stabilized (fixed to pylon); will be 1.0 if stabilized with respect to the aircraft or wing (see figure 3f)
q	dynamic pressure, lb/sq-ft
S	wing area (116 sq ft), sq-ft
T	total thrust obtained as the difference between rotor on and rotor off drag for corresponding α, V and mount configuration, lb
V	freestream airspeed, knots
α	angle of attack of the fuselage reference line (see figure 2a), deg
β	rotor flapping; positive with blade flapping forward, deg
δ_3	pitch flap coupling ratio, $\tan \delta_3 = - \partial\theta / \partial\beta$, deg

ϵ swashplate retardation (see reference 4); positive when the swashplate is rotated in a direction opposite to rotor rotation, deg

ζ ratio of measured damping to critical damping (see figure 6 for derivation); expressed as either a ratio or percent critical

θ blade pitch, deg

ϕ_x and ϕ_y pylon angular displacements in pitch and yaw respectively; positive when XV-3 right pylon is down and inboard, deg

ψ blade azimuth location; 0 when blade is vertically up, deg

ω_x and ω_y pylon static natural frequencies in pitch and yaw respectively, per sec

Ω rotor speed, rpm

AIRCRAFT AND EQUIPMENT

Aircraft Details and Mounting

The XV-3 is shown in figures 1(a) and (b) mounted in the 40- by 80-foot wind tunnel with the wing mount and the roll free installations respectively. Sketches of the XV-3 and roll free mount arrangements are presented in figure 2. A summary of geometric data for the aircraft is presented in Table I. A list of the configurations tested is shown in Table II. The pylons were fixed in the horizontal or airplane position for all the tests.

The wing mount installation in the wind tunnel was identical to that used for the tests of reference 1. A sketch of the roll free mount presented in figure 2(b) shows the relative position of the roll axis and the aircraft. Limits in roll of the aircraft were $\pm 3^{\circ}$. The aircraft was restrained in roll by Lord mounts resulting in a system static natural frequency in roll of 0.5 cycles/sec. A solenoid actuated locking pin was used to center the model in a static condition.

Swashplate, Hub and Pylon

The primary changes made to the original XV-3 rotor-pylon support system are described in the following paragraphs. Detail photographs of the right pylon-hub assembly and diagrams of the swashplate stabilization or coupling linkage and pylon restraint arrangements are shown in figures 3(a) through 3(g).

Swashplate Modifications.- The swashplate was modified for the present tests by moving it from a position forward of the hub to the present position near the transmission. The cyclic pitch control was disconnected and the swashplate was connected to the blades through arms mounted on the end of the collective pitch tube. (See figure 3c.) Provisions were made to obtain nominal values of 20 and 35° of δ_3 and swashplate retardation, ϵ . Retardation was obtained by re-indexing the rotating part of the swashplate with respect to the hub in a direction opposite to rotor rotation.

Swashplate Stabilization.- The swashplate was stabilized by coupling the swashplate to the wing or fuselage as illustrated in the sketches of figure 3(f) (for wing coupling).

As shown in figure 3(g), the swashplate was moved in the pitch direction through a fast-response hydraulic boost. Swashplate stabilization, k_x (or k_y), could be set by choosing proper combinations of connecting rod positions on the bell cranks. A torque tube running through the wing to the fuselage enabled the coupling of the swashplate to the fuselage. The swashplate was coupled to the wing tip rather than the fuselage after it was found that relative wing-tip-fuselage motion in torsion was negligible. With wing stabilization, the rear connecting rod was attached at the pivot point of the rear bell crank. The swashplate was coupled to the wing without hydraulic boost in the yaw direction.

Hub and Pylon Restraint.- Hub restraint was obtained by installation of torque springs in line with the flapping hinge.

The original XV-3 pylon actuator mounts and the bases for the dampers and Lord mounts were reinforced. During the tests, pylon stiffness was changed by interchanging Lord mounts of different stiffness. Pylon mount damping was changed by adjustment of the viscous dampers. The dampers were removed for a major part of the testing because the flexibility in their mounts complicated the evaluation of both the mechanical damping and stiffness of the system.

Pylon Actuators.- An hydrualic actuator was installed in the right pylon restraint linkage as shown in figures 3(e) and (g). Statically the hydraulic actuator could pulse the pylon up $1\text{-}1/2^{\circ}$ and back again

with step inputs. The pylon conversion actuator was used to pulse the pylon for test configurations and conditions where the rotor was heavily damped.

TESTS AND PROCEDURE

Table II is an index to the test runs and aircraft configurations. Before power-on testing was done on either support system, the blades were removed and basic aerodynamic data were obtained for an angle-of-attack range of about -5 to 6° and for the full range of airspeeds to be used with the blades on. The blades-on tests were made at airspeeds between 40 and 195 knots with the rotor speed set at 324 rpm and angle of attack at -2°. Rotor speed was varied from 280 to 400 rpm for selected airspeeds. The angle-of-attack range was -5 to 5°.

For each configuration, the angle-of-attack, rotor thrust and rotor speed were held constant while the airspeed was increased. When the target values of airspeed were reached, angle-of-attack, rotor speed and rotor thrust were set and steady-state six-component force and moment data were recorded using the wind tunnel balance system. The oscillographs were started and the pylon was pulsed with either the hydraulic actuator or the pylon conversion actuator. Direct writing oscillographs were used in order to evaluate pylon damping, frequency, and rotor component loads prior to advancing to the next test condition. For some configurations and airspeeds, angle-of-attack, rotor thrust and rotor speed were varied individually.

DATA ACQUISITION AND REDUCTION

The measurements obtained during the tests consisted of 6-component force and moment data obtained from the wind tunnel balance system, and oscillograph data for the positions and loads listed in Table III. Movies on the right pylon motion were made for most of the high speed tests as well as for all low damped pylon oscillations.

Thrust was evaluated from the wind tunnel force data by subtracting power-on drag from the blades-off drag value for corresponding angles-of-attack and dynamic pressure.

The values of pylon damping ratio used in this report were obtained graphically as indicated in figure 4. The method is essentially a comparison of the measured rate of decay with that calculated for a one-degree-of-freedom spring-mass-damper system. A principal limitation of the method is that damping above 15% critical could not be evaluated accurately and the data for these cases are presently being reduced using computer techniques.

RESULTS

Time histories of pylon displacement and rotor flapping are shown in figures 5 and 6 for several test conditions. The conditions chosen indicate the effect of changes in swashplate coupling on the rate of decay of the right pylon oscillation after the pylon was pulsed. The dashed lines on the displacement traces represent the backward whirl or

low frequency mode for which an increase in damping was a primary objective of the test program. The forward whirl mode may be seen for the lower values of swashplate stabilization as a higher frequency component superimposed on the lower frequency oscillations.

The damping ratios (in terms of % critical damping, see Figure 4) of the backward whirl mode are presented as functions of airspeed in figures 7 to 11. Damping as a function of thrust is presented in figure 12. As may be seen from the figures, crossover speeds or airspeeds for neutral stability were not obtained for some of the configurations. Since the damping deteriorated abruptly before reaching a crossover speed, several of the test runs were terminated as soon as any reduction in damping was noticed. The data points corresponding to damping above 15% critical were noted on the plots by the symbols at 15% critical damping with arrows attached. Frequencies shown for high damping are based on estimations for the time to complete one-half cycle.

In summary, the results substantiate the theoretical predictions of reference 4, namely that increases in damping of the low frequency backward whirl mode can be obtained with swashplate stabilization, increase in pylon stiffness or with hub restraint. Increasing thrust was stabilizing.

REFERENCES

1. Koenig, David G., Greif, Richard K., and Kelly, Mark W.: Full-Scale Wind-Tunnel Investigation of the Longitudinal Characteristics of a Tilting-Rotor Convertiplane.

2. Deckert, Wallace H., and Ferry, Robert G.: Limited Flight Evaluation of the XV-3 Aircraft. AFFTC TR-60-4, May, 1960.

3. Quigley, Harvey C., and Koenig, David G.: The Effect of Blade Flapping on the Dynamic Stability of a Tilting-Rotor Convertiplane. TND-778.

4. Hall, Jr., W. Earl: Prop-rotor Stability at High Advance Ratios. Journal of American Helicopter Society. June, 1966.

TABLE I - GEOMETRIC DATA

Wing	
Reference area - sq ft	116.0
Span (distance between pylons) ft	29.5
Aspect ratio	7.8
Incidence, deg	5
Airfoil section	NACA 23021
Fuselage	
Length, ft	30.33
Depth, ft	5.31
Maximum width, ft	4.05
Rotor (2 blades)	
Diameter, ft	21.0
Blade section	NACA 0015
Chord, in	11.0
Solidity	.056
Blade twist deg/ft radius	-1.60
Power	
Engine (USAF designation)	R-985
Engine rating (hp/rpm/alt)	450/2300/2300
Rotor engine speed ratio	7.12 :1

TABLE II.- INDEX TO THE TESTS

Test run	Model Support	δ_3/ϵ	Hub restraint K_b	Pylon Stiffness Pitch ω_x	Pylon Stiffness Yaw ω_y	Pylon Damper reference setting Pitch	Pylon Damper reference setting Yaw	Swashplate * Coupling k_x	Swashplate * Coupling k_y
3 to 6	Wing	22°/24.2°	0	3.4	6.6	1/16 turn	2 turn RH 1/2 " LH	1.0_{FUS}	1.0
7 & 8	↓	↓	740	↓	↓	↓	↓	1.0	↓
9	↓	↓	0	↓	3.8 R.H. 3.5 L.H.	↓	↓	-.5	-.5
10	↓	↓	↓	2.5	3.8	Dampers off	2 turn	↓	↓
11	↓	↓	↓	↓	↓	↓	↓	1.0	↓
12	↓	↓	740	↓	↓	↓	↓	-.5	↓
13	↓	↓	0	3.2 (right)	↓	5 turn R.H. 1/16 " L.H.	↓	↓	↓
14	↓	↓	↓	3.4 (right	↓	1/16 turn	↓	↓	↓
15	↓	↓	↓	↓	3.5	↓	1/2 turn	0	0
16	↓	↓	↓	↓	↓	↓	↓	1.0	1.0
17	↓	35°/31.1°	↓	2.5	↓	Dampers off	↓	-.5	-.5
19	Fuselage	↓	↓	2.0	↓	↓	↓	↓	↓
20	↓	↓	↓	↓	↓	↓	↓	0	0
21	↓	↓	740	↓	↓	↓	↓	↓	↓
22	↓	↓	0	↓	↓	↓	↓	1.0	1.0
23 & 24	↓	↓	↓	2.3	6	5 turns	Dampers off	1.5	0
25	↓	↓	↓	2.5	↓	1/16 turn	↓	↓	↓

* Pylon is coupled to wing unless noted as $(\ )_{FUS}$ for fuselage coupling.

TABLE III PYLON-ROTOR MEASUREMENTS

POSITIONS

PYLON POSITION IN PITCH	BOTH SIDES
PYLON POSITION IN YAW	
WING TIP VERTICAL ACCELERATION	
SWASHPLATE POSITION - PITCH	
SWASHPLATE POSITION - YAW	
WING TIP TORSION POSITION (FUSELAGE AS REFERENCE)	
ROTOR FLAPPING	
BLADE COLLECTIVE PITCH TUBE POSITION	
AIRCRAFT POSITION IN ROLL	
BLADE FEATHERING (CYCLIC)	LEFT SIDE

LOADS

PITCH LINKS	RIGHT SIDE
BLADE BEAM BENDING*	
BLADE CHORD BENDING*	
MAST BENDING	BOTH SIDES
MAST TORQUE	RIGHT SIDE
BLADE DRAG BRACE	BOTH SIDES
PYLON RESTRAINT FORCE IN PITCH	RIGHT SIDE
HUB YOKE BEAM BENDING	BOTH SIDES
PITCH CYCLIC CONTROL FORCE	
YAW CYCLIC CONTROL FORCE	
PITCH CYCLIC CLEVIS BENDING	

* 2.50 FT FROM MAST CENTER

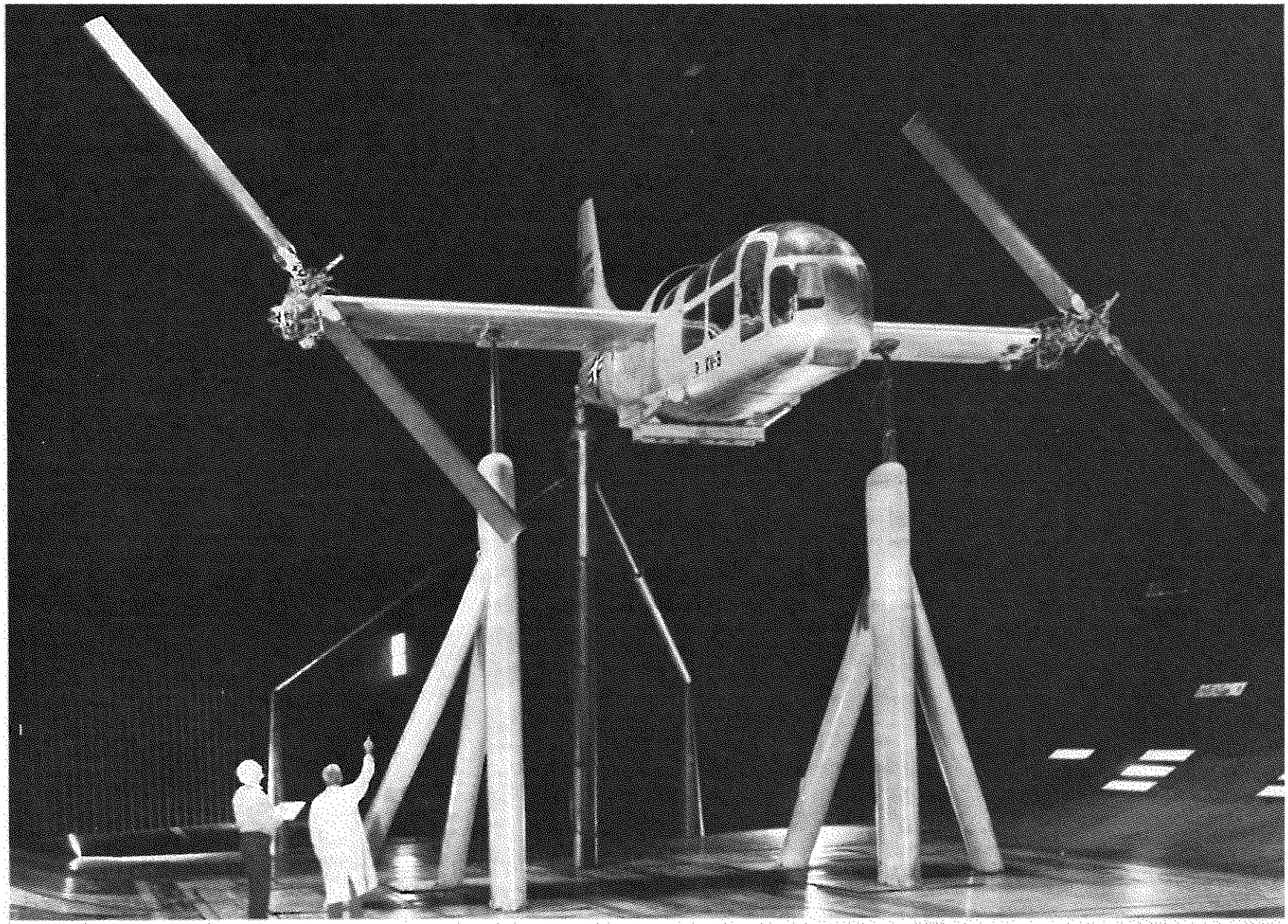

(a) Wing mount.

Figure 1.- The XV-3 mounted in the Ames 40- by 80-Foot Wind Tunnel.

NATIONAL AERONAUTICS AND SPACE ADMINISTRATION
AMES RESEARCH CENTER, MOFFETT FIELD, CALIFORNIA

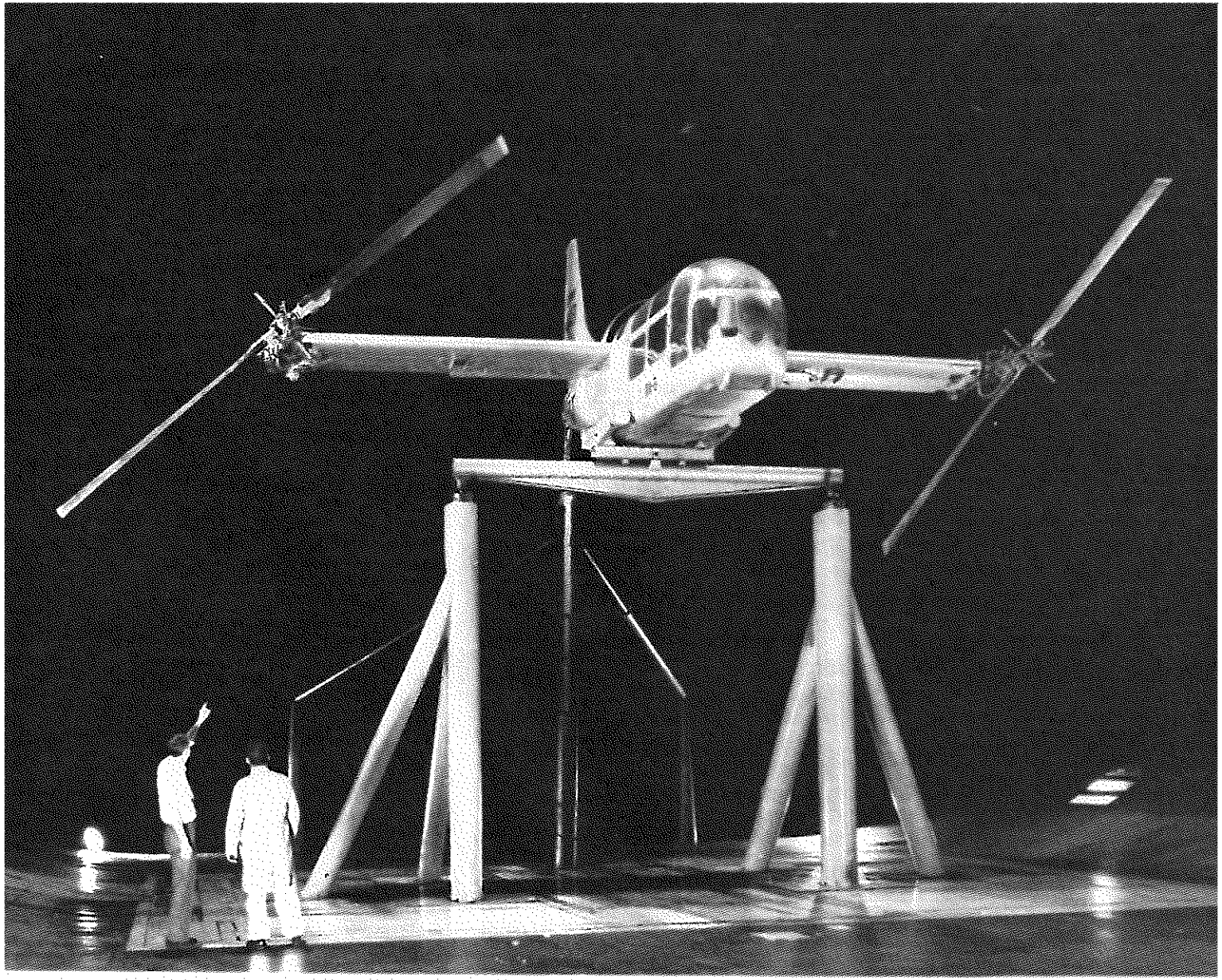

(b) Fuselage Mount.

Figure 1.- Concluded.

NATIONAL AERONAUTICS AND SPACE ADMINISTRATION
AMES RESEARCH CENTER, MOFFETT FIELD, CALIFORNIA

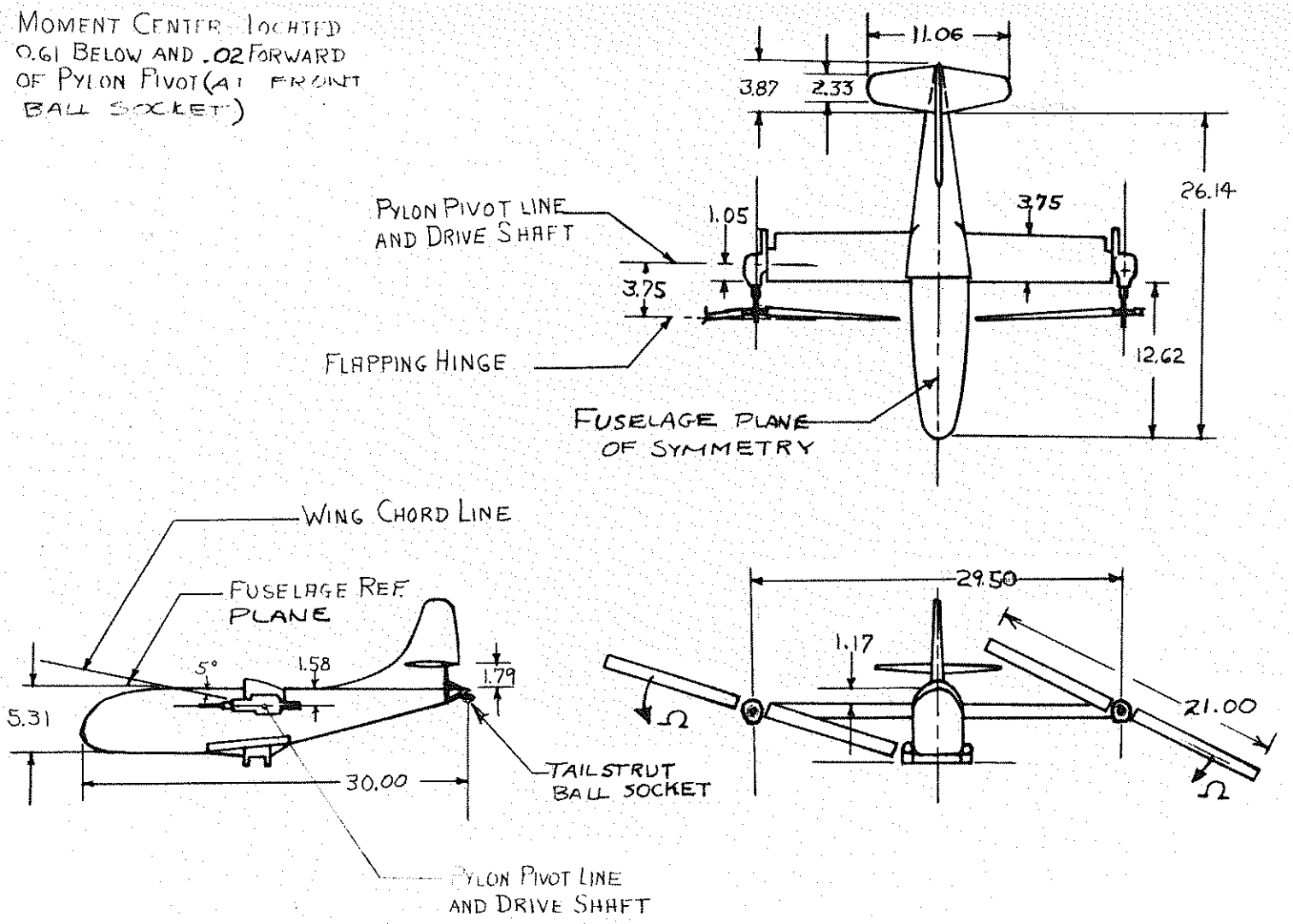

(a) Aircraft three view (Dimensions in feet)

Figure 2.- Sketches.

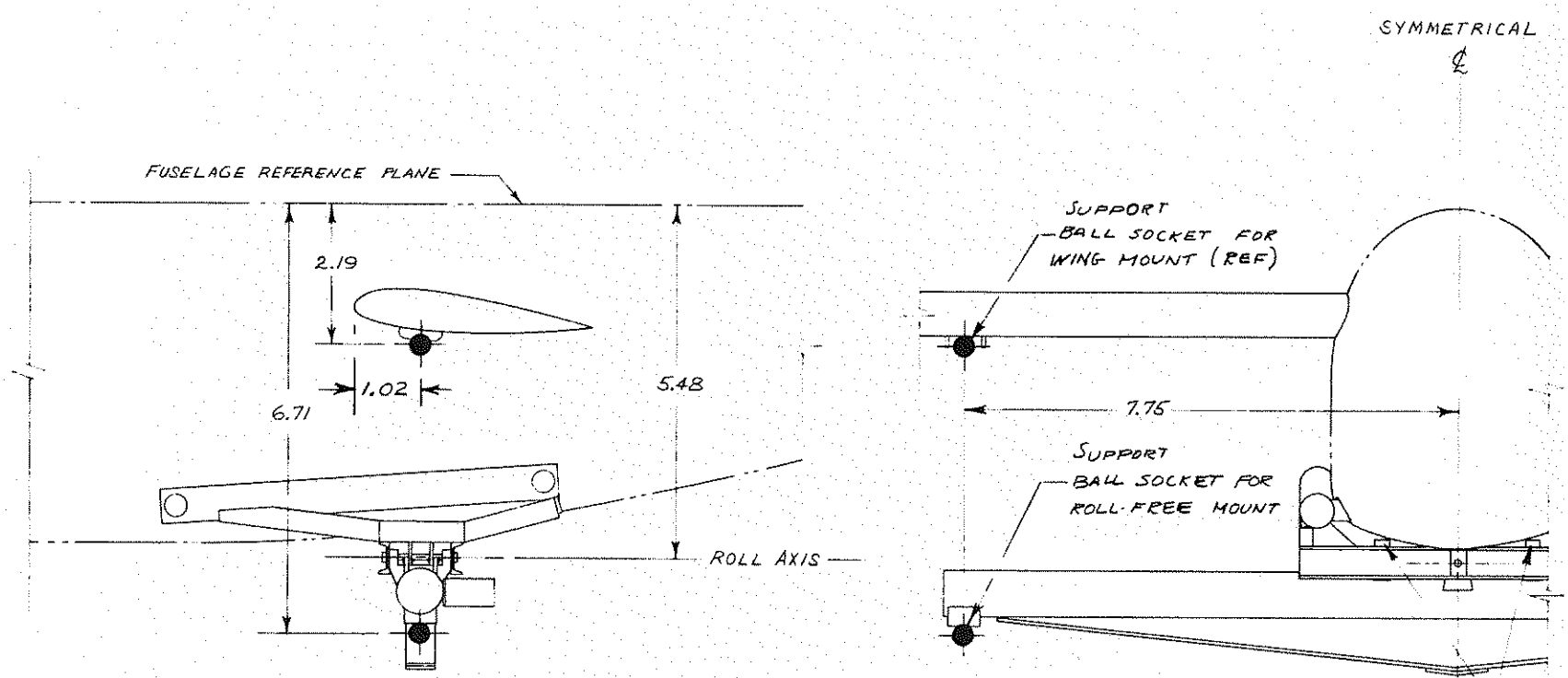

(b) Details of roll-free mount

Figure 2.- Concluded.

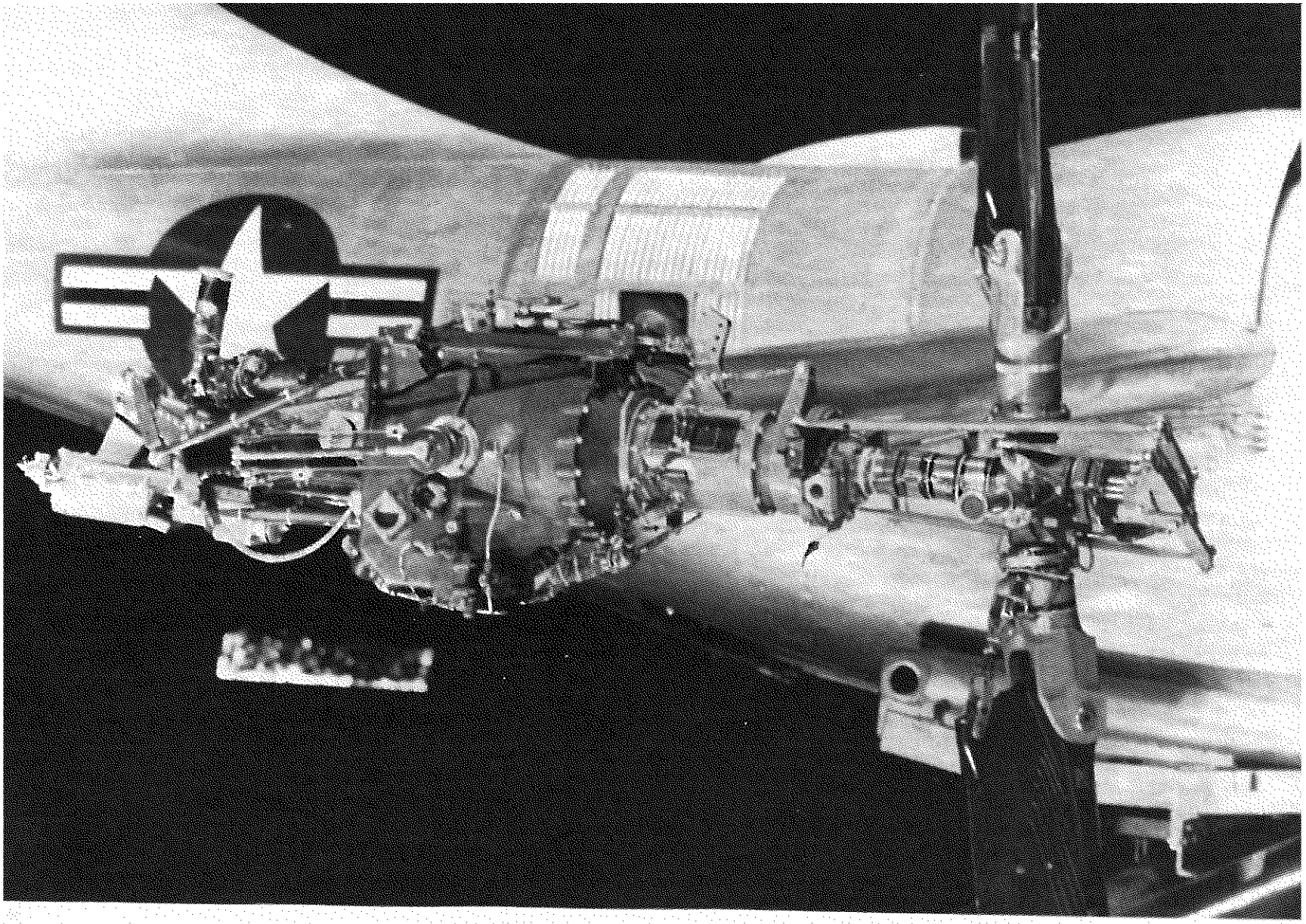

(a) Looking inboard; pitch damper disconnected.

Figure 3.- Detail views of the right pylon-rotor assembly.

NATIONAL AERONAUTICS AND SPACE ADMINISTRATION
AMES RESEARCH CENTER, MOFFETT FIELD, CALIFORNIA

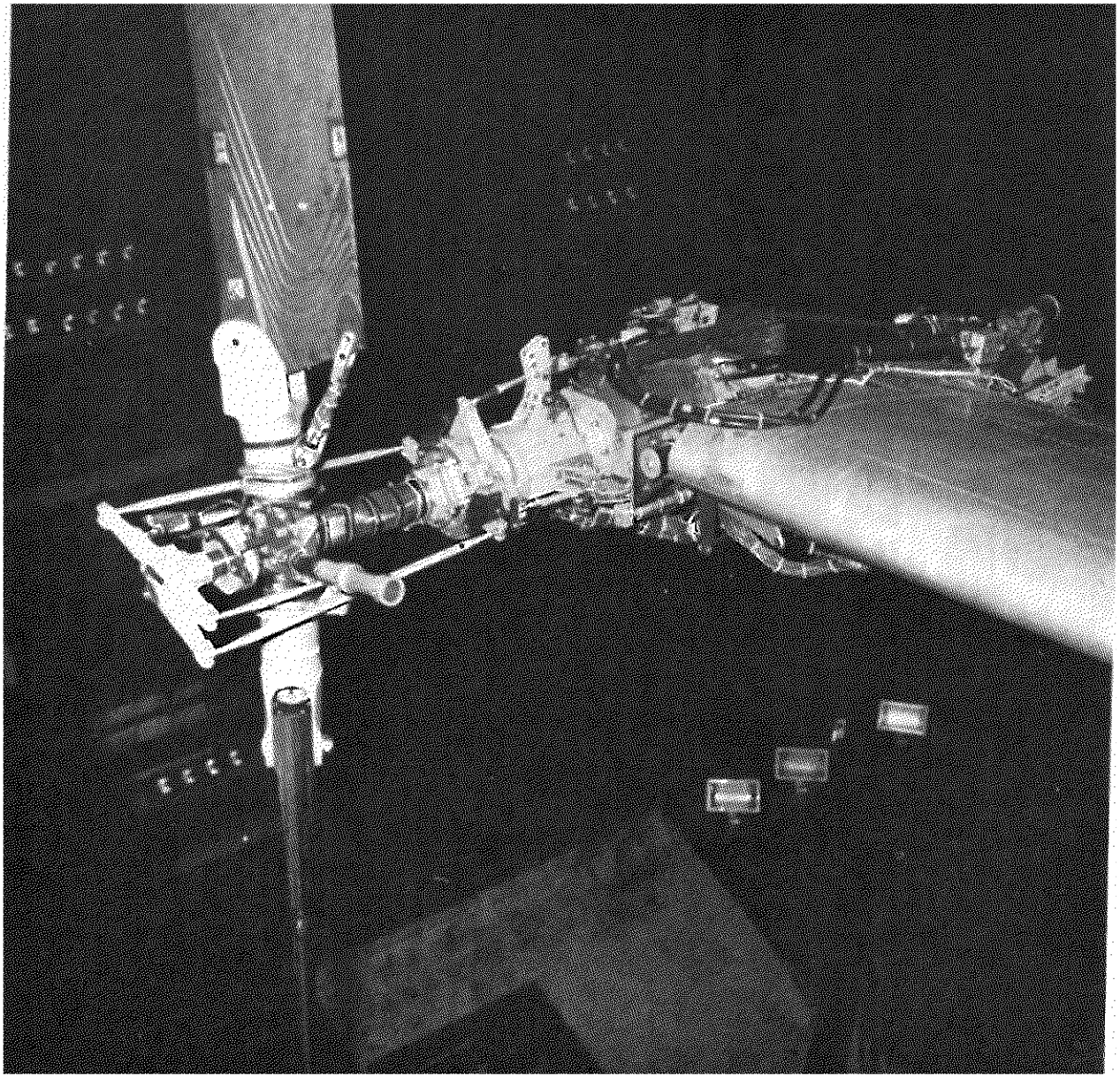

(b) Looking outboard; pitch damper connected.

Figure 3.- Continued.

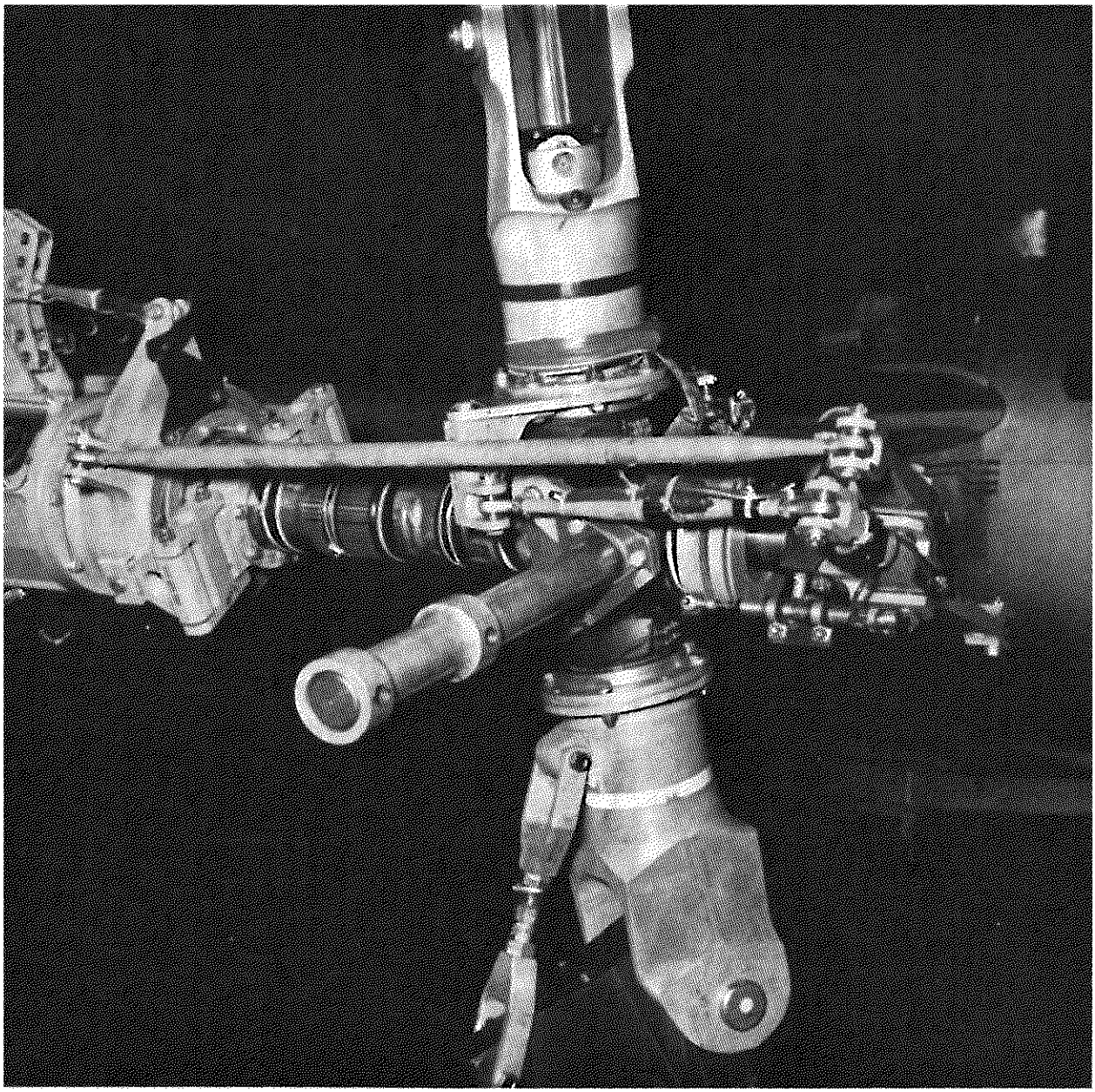

(c) Hub-swashplate assembly.

Figure 3.- Continued.

(c) Pylon transmission assembly.

Figure 3.- Continued.

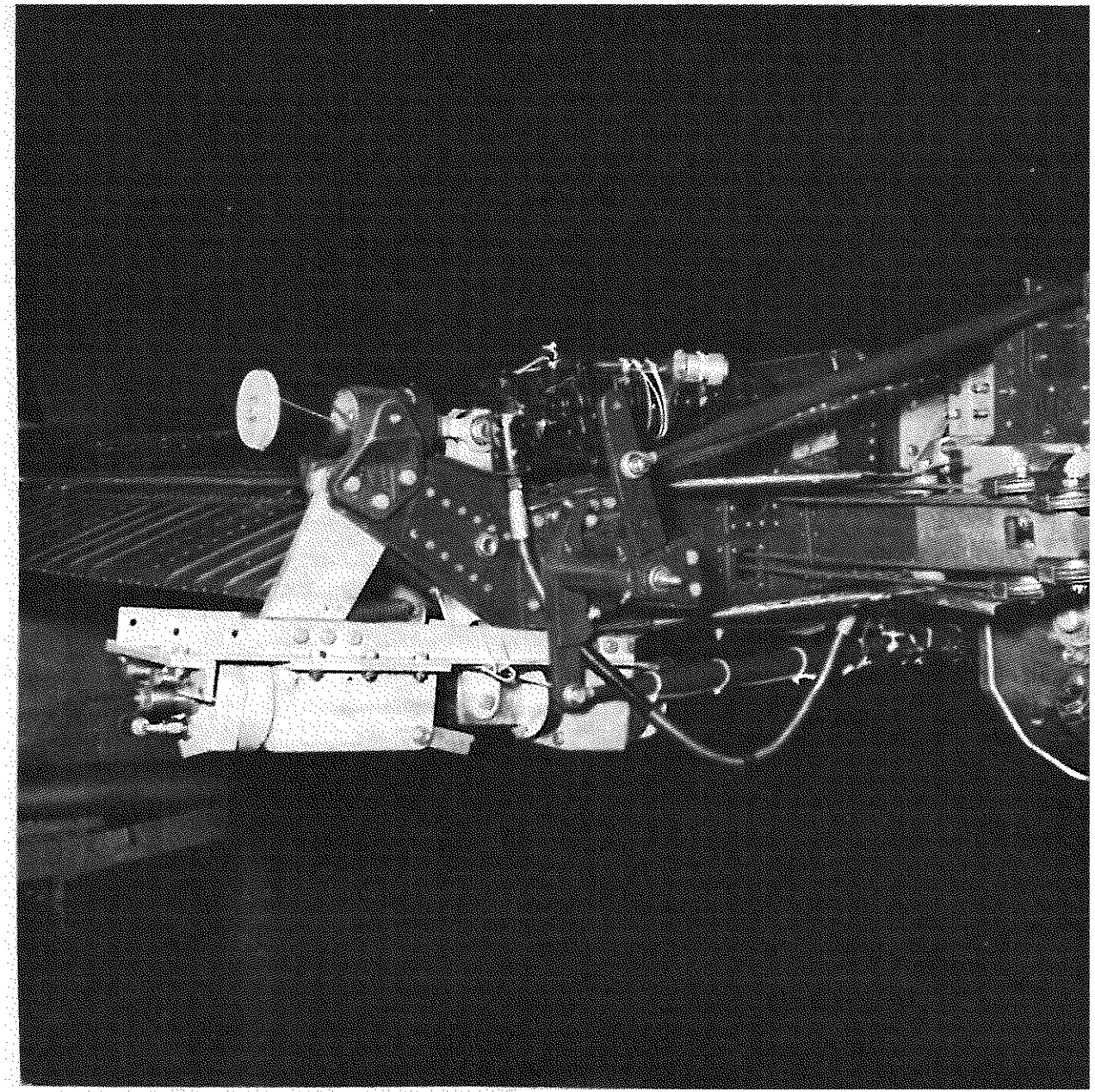

(e) Aft pylon wing tip assembly.

Figure 3. Continued

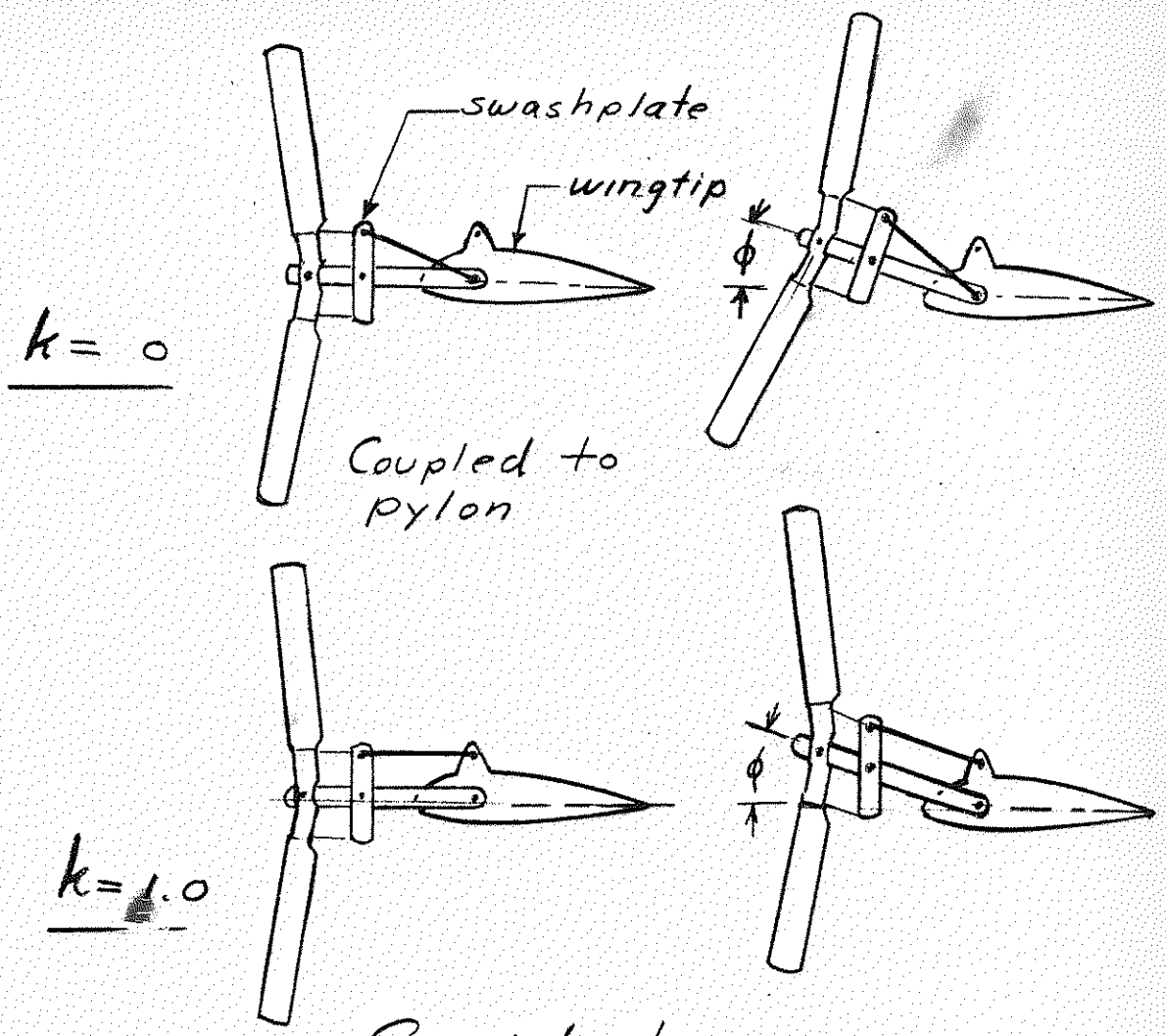

(f) Swashplate stabilization.

Figure 3.- Continued.

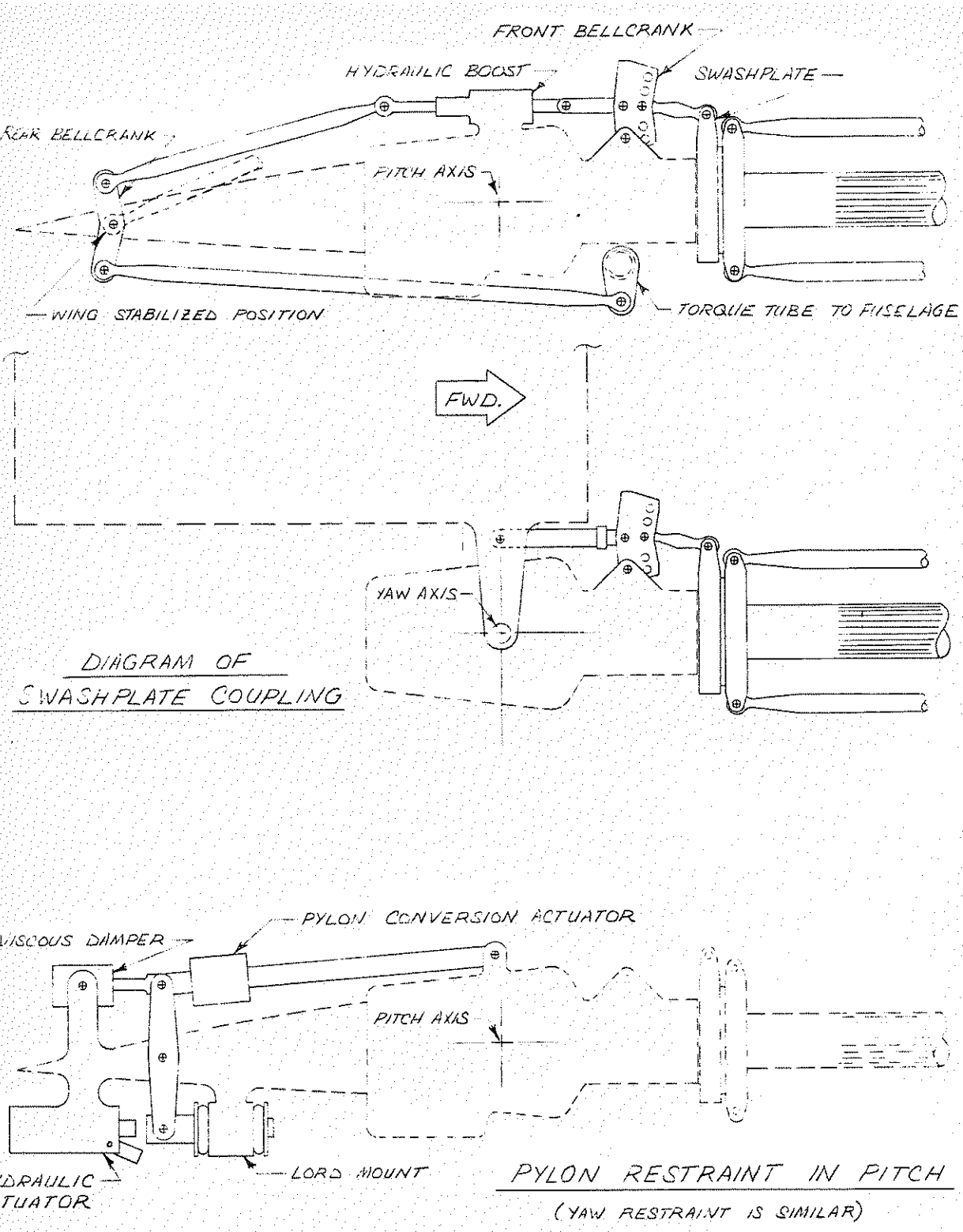

(9) Swashplate Coupling and Pylon Restraint

Figure 3.— Concluded.

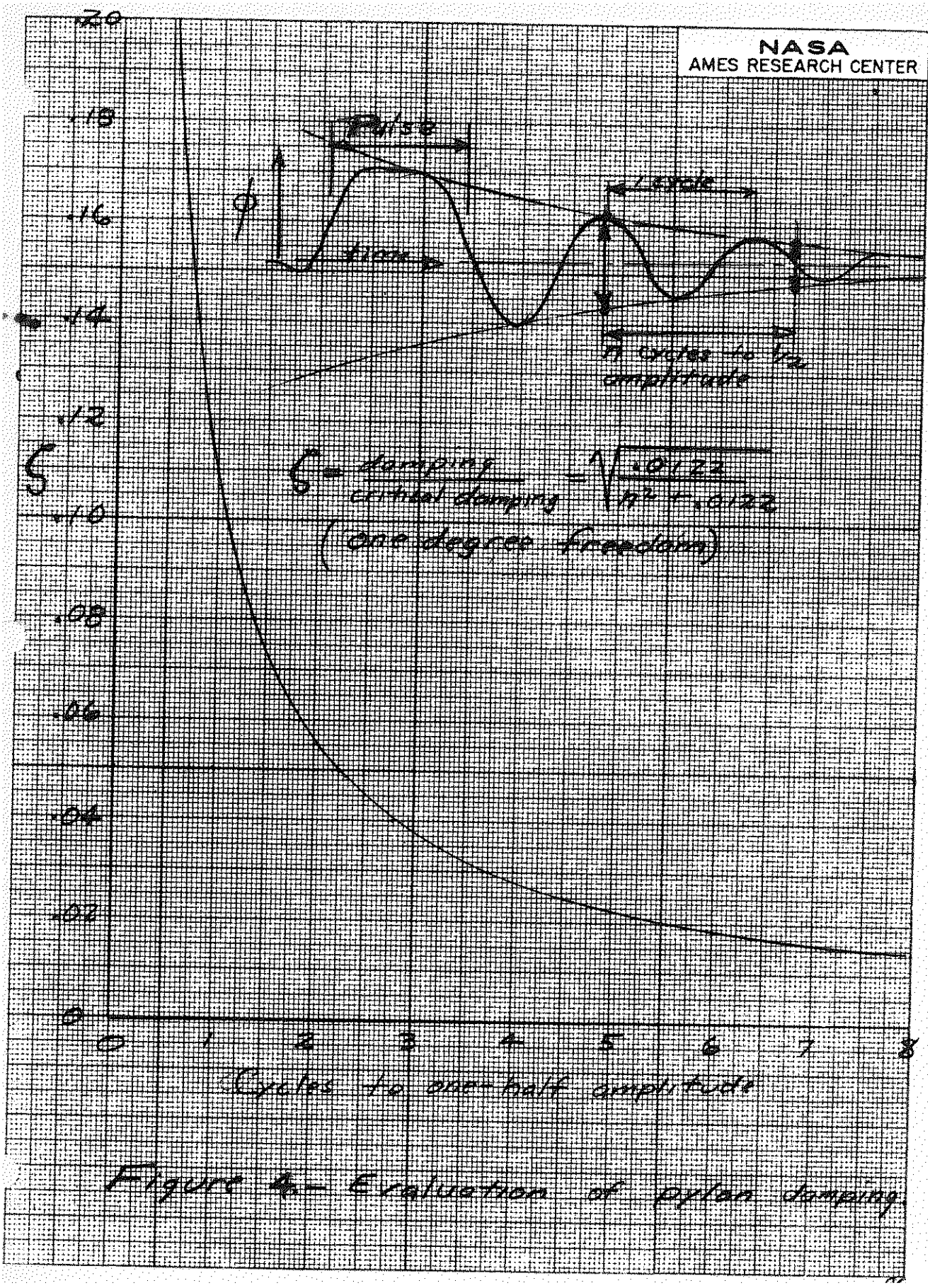

Figure 4.— Evaluation of system damping.

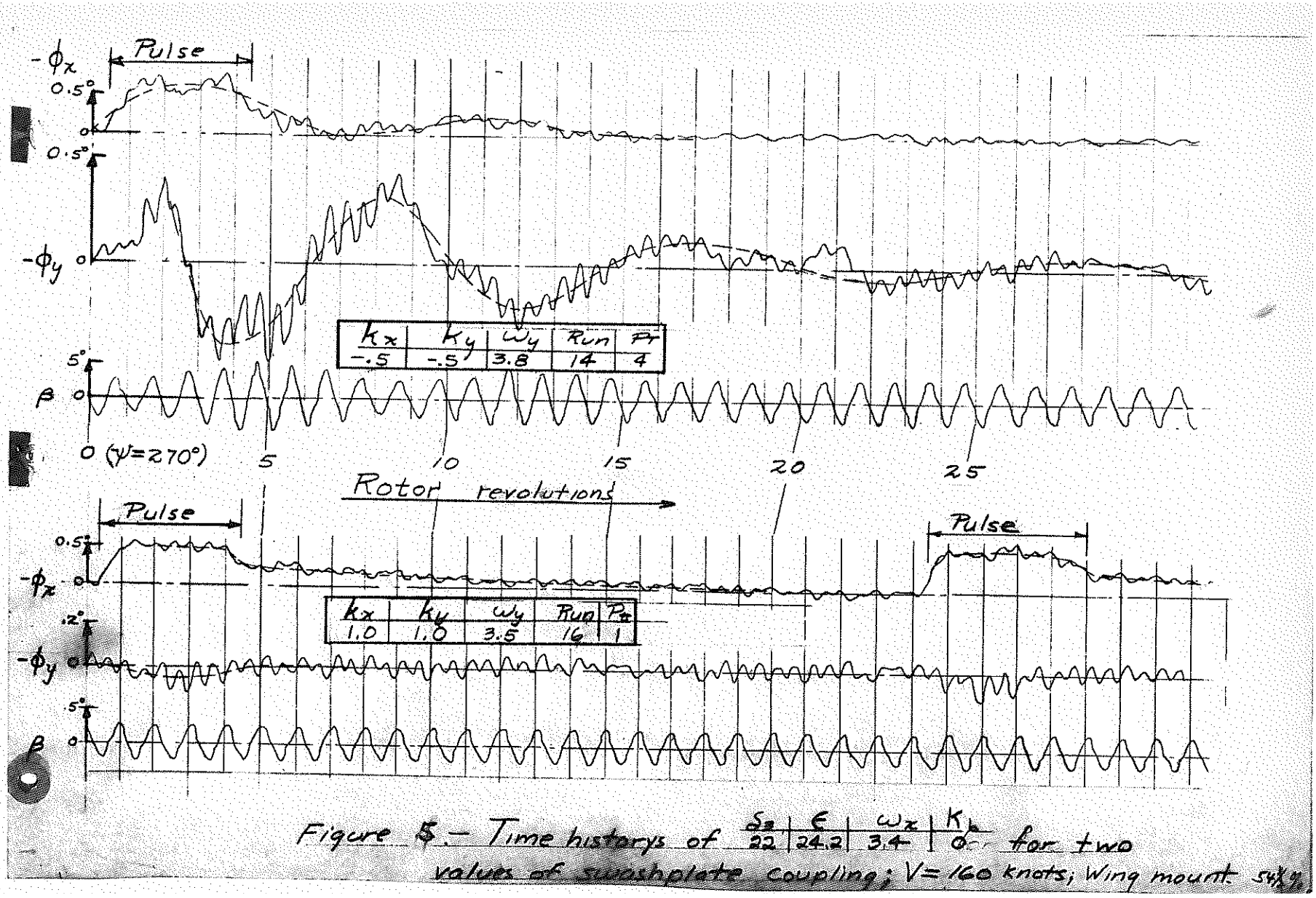

k_x	k_y	ω_y	Run	Pr
-.5	-.5	3.8	14	4

k_x	k_y	ω_y	Run	Pr
1.0	1.0	3.5	16	1

Figure 5.— Time historys of $\frac{\delta_3}{22}$ | $\frac{\epsilon}{24.2}$ | $\frac{\omega_x}{3.4}$ | $\frac{K}{0}$ for two values of swashplate coupling; V = 160 knots; Wing mount 54% g

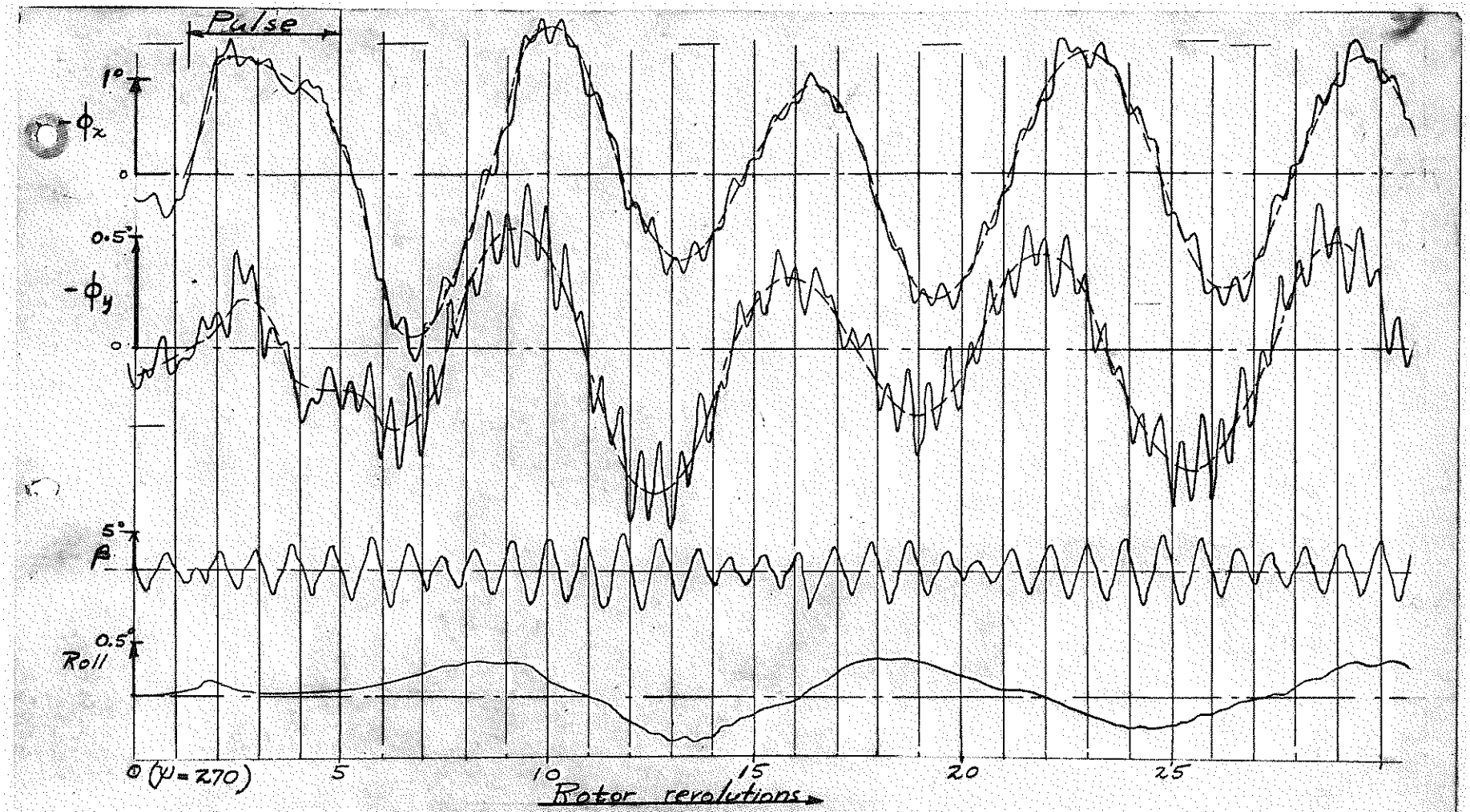

(a)

k_x	k_y	V	Run	Pt
0	0	125	20	19

δ_3	ϵ	ω_x	ω_y	k_b
35°	31.1°	2.0	3.5	0

Figure 6.-Time historys for, with and without swashplate coupling; fuselage mount.

549

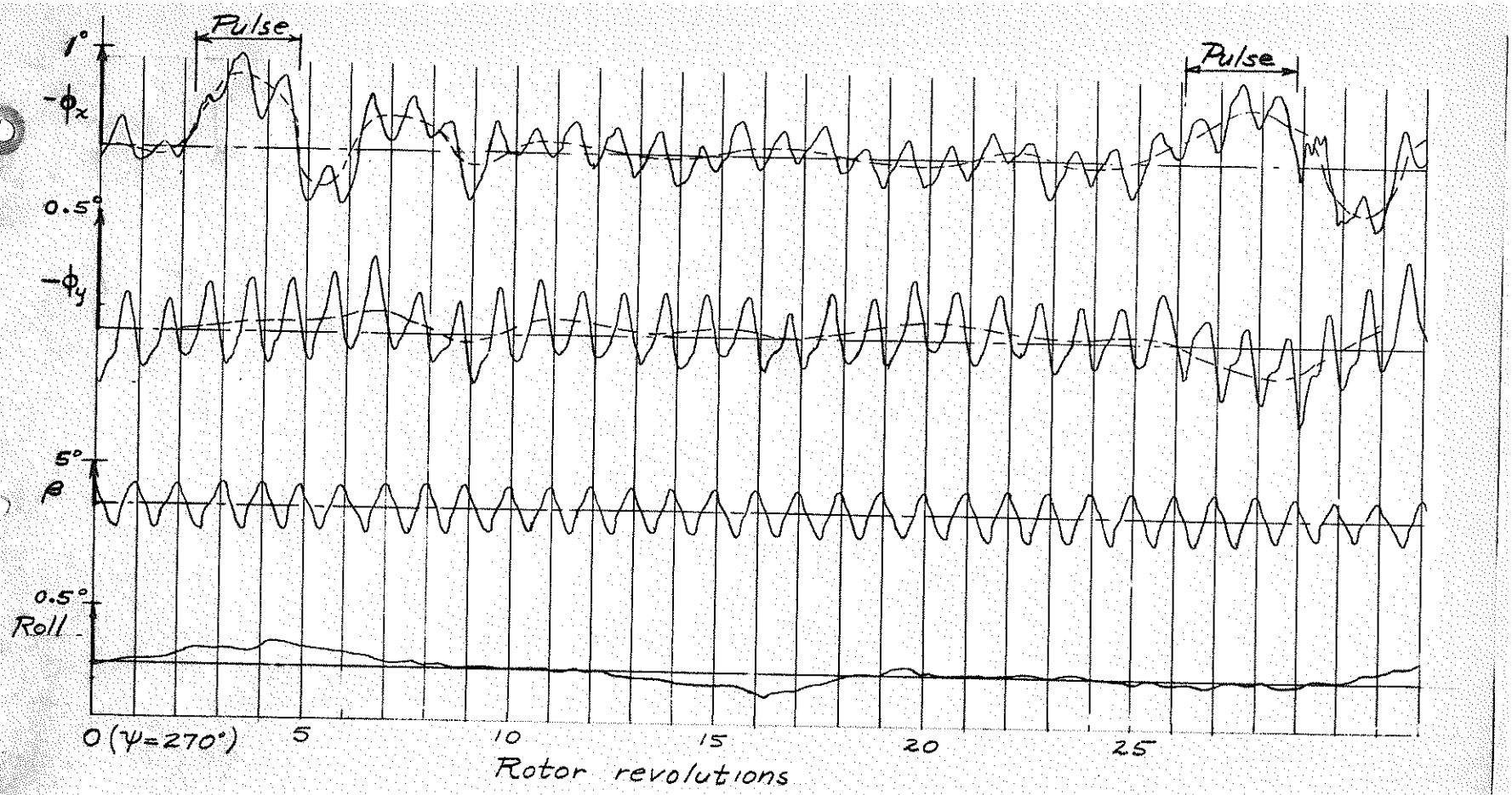

(b)

k_x	k_y	V	Run	Pt
1.0	1.0	170	22	5

Figure 6.- Concluded.

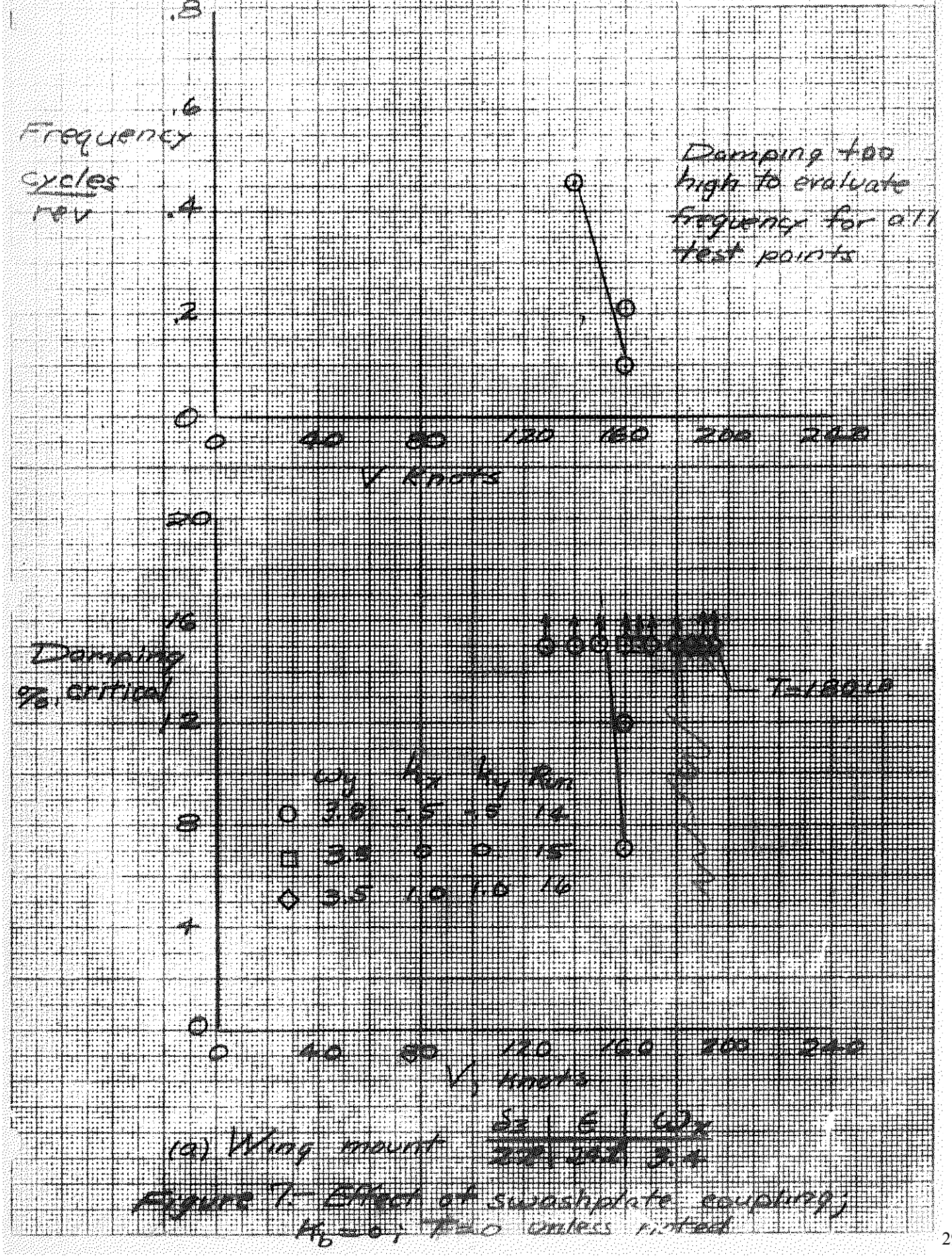

(a) Wing mount $\frac{\Omega z}{2\pi}$ | $\frac{\omega}{2\pi}$ | $\frac{\omega_{2x}}{2\pi}$ 3.4

Figure 7. Effect of swashplate coupling, $K_b = 0$, $T = 0$ unless noted.

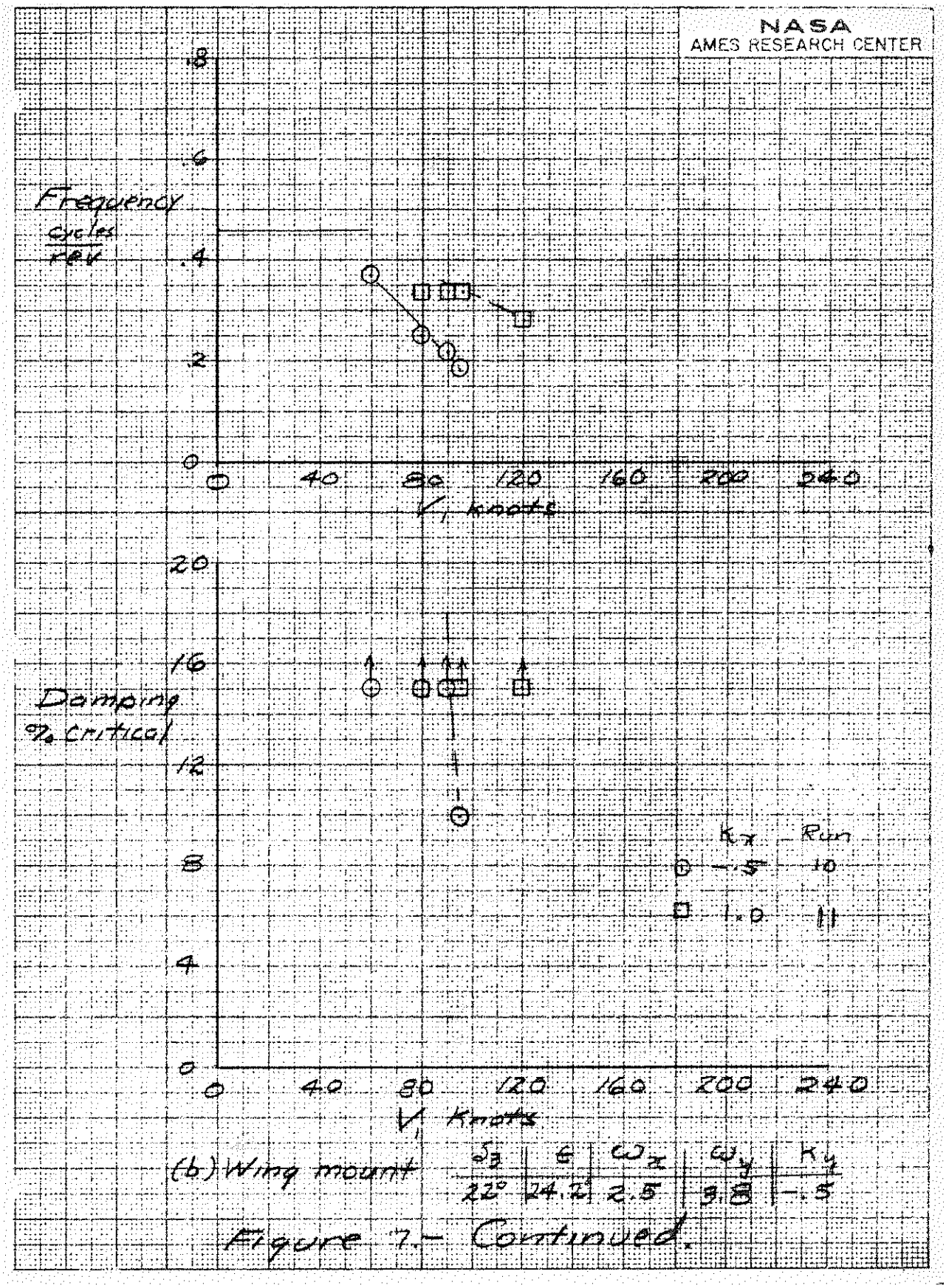

(b) Wing mount

δ_3	ϵ	ω_x	ω_y	K_y
22°	24.2	2.5	3.8	-.5

Figure 7.– Continued.

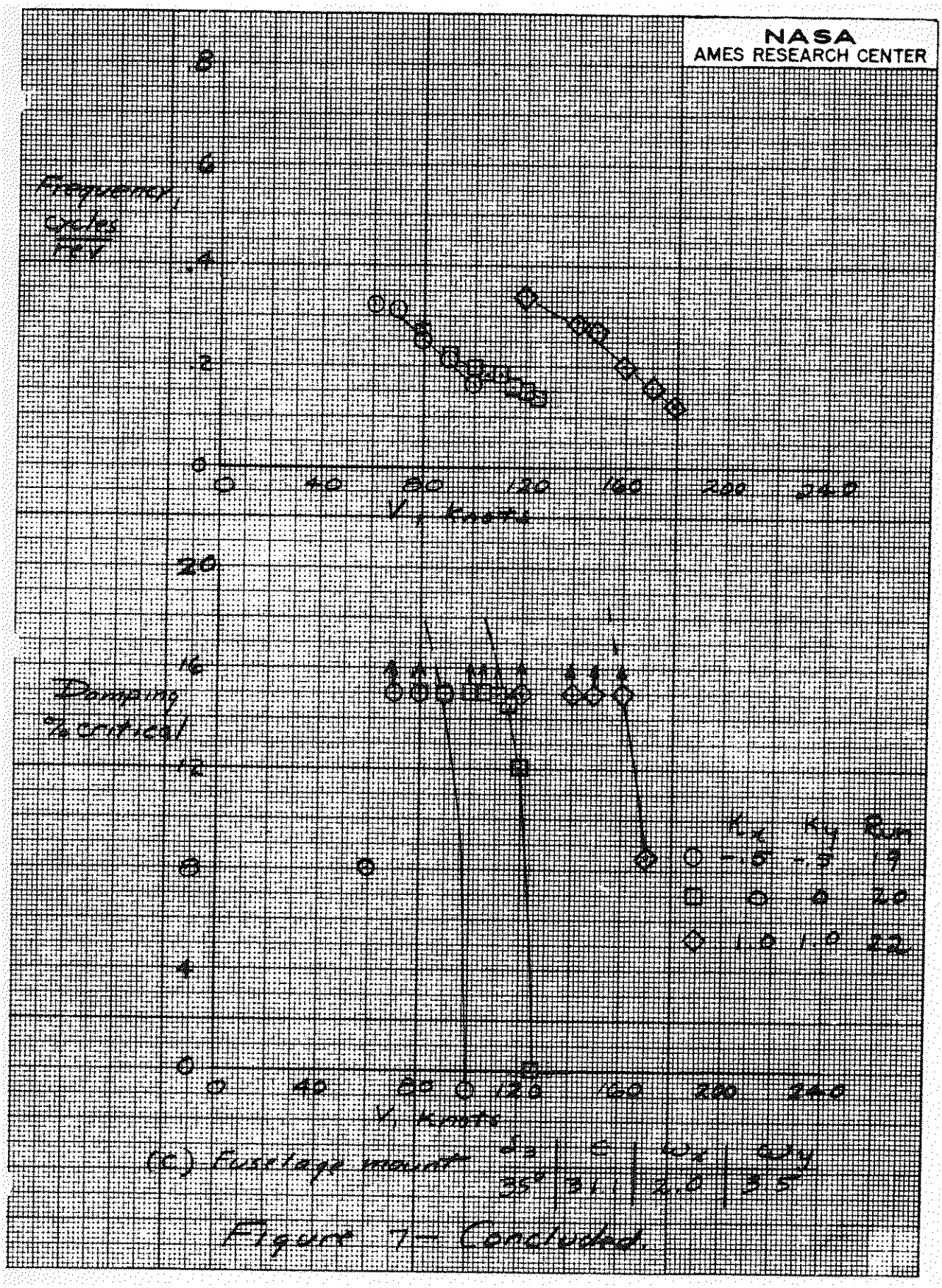

Figure 7.— Concluded.

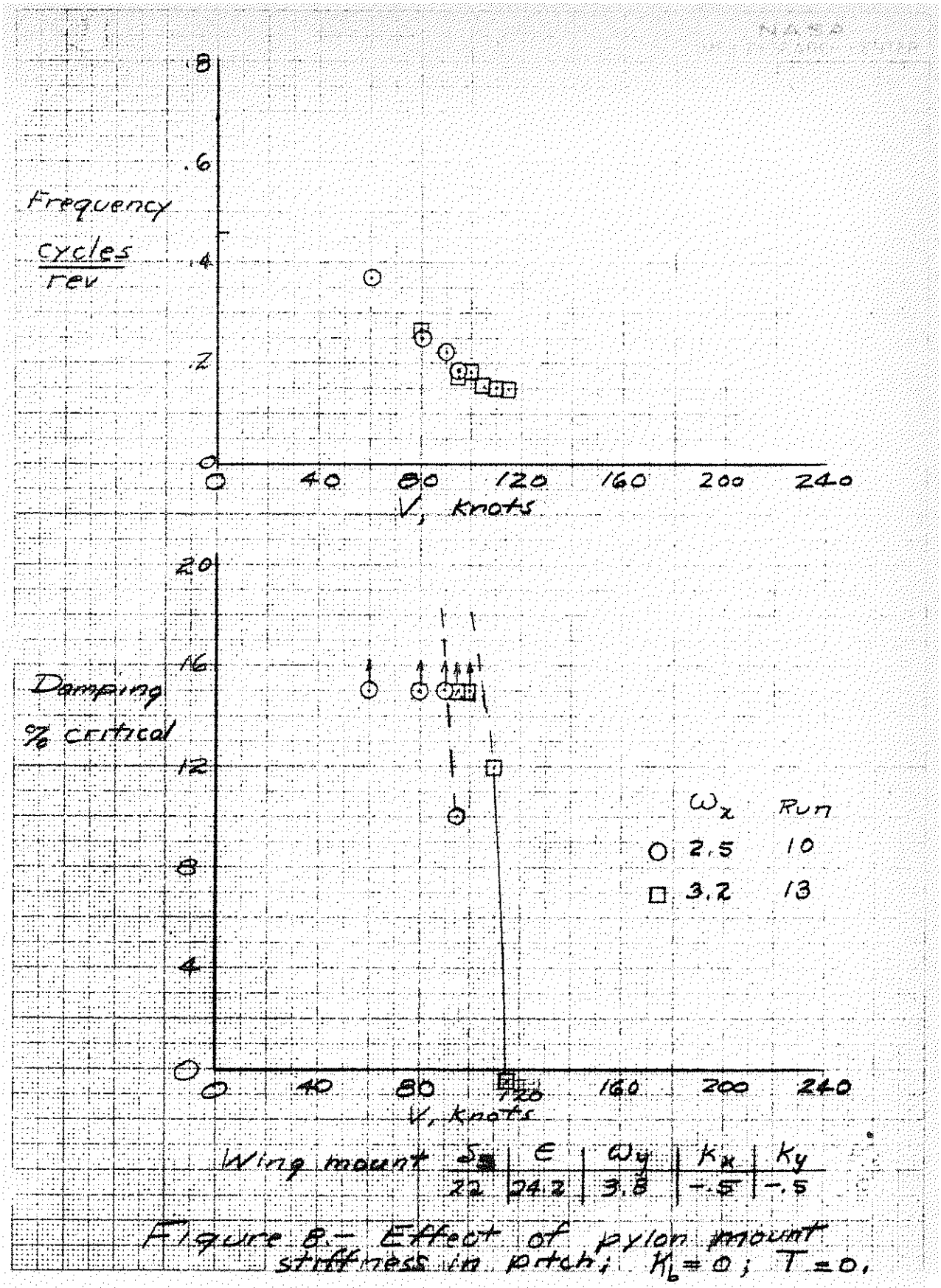

Figure 8.— Effect of pylon mount stiffness in pitch; $K_b = 0$; $T = 0$.

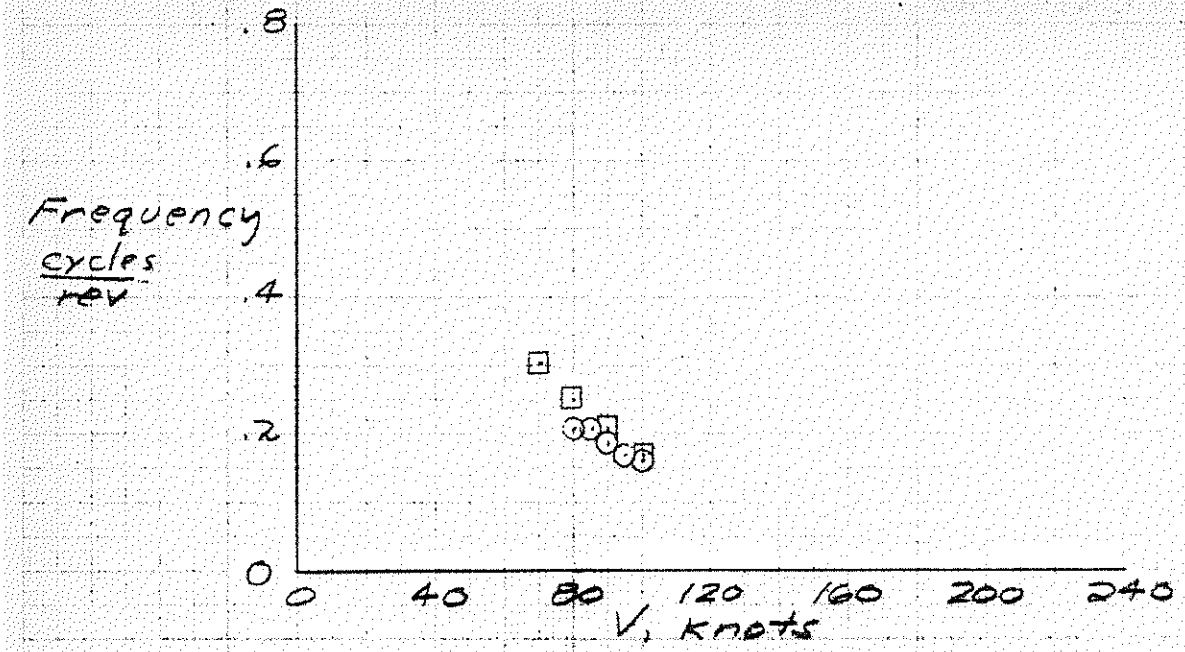

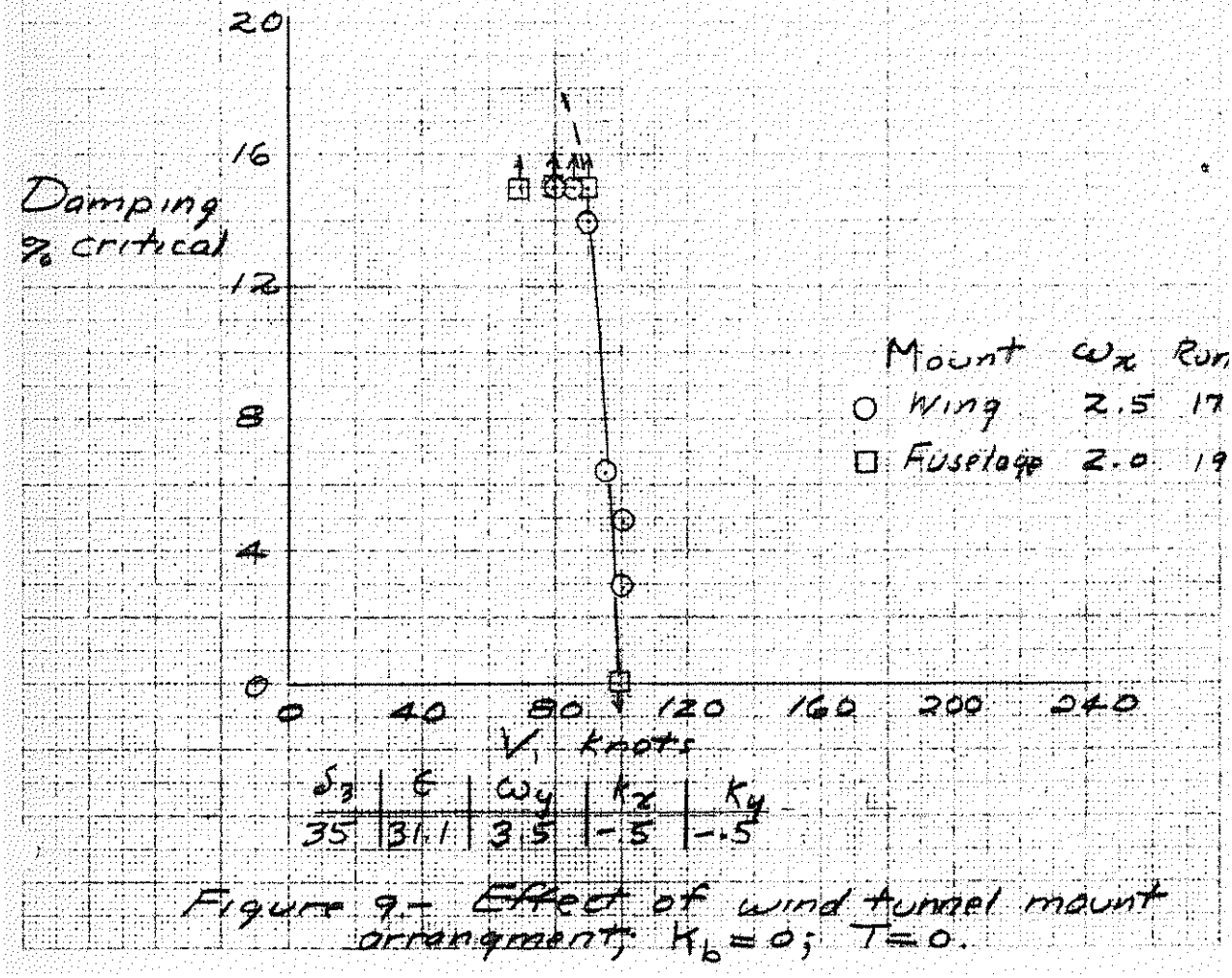

S_3	ϵ	ω_y	K_x	K_y
35	31.1	3.5	-.5	-.5

Figure 9.- Effect of wind tunnel mount arrangement; $K_b = 0$; $T = 0$.

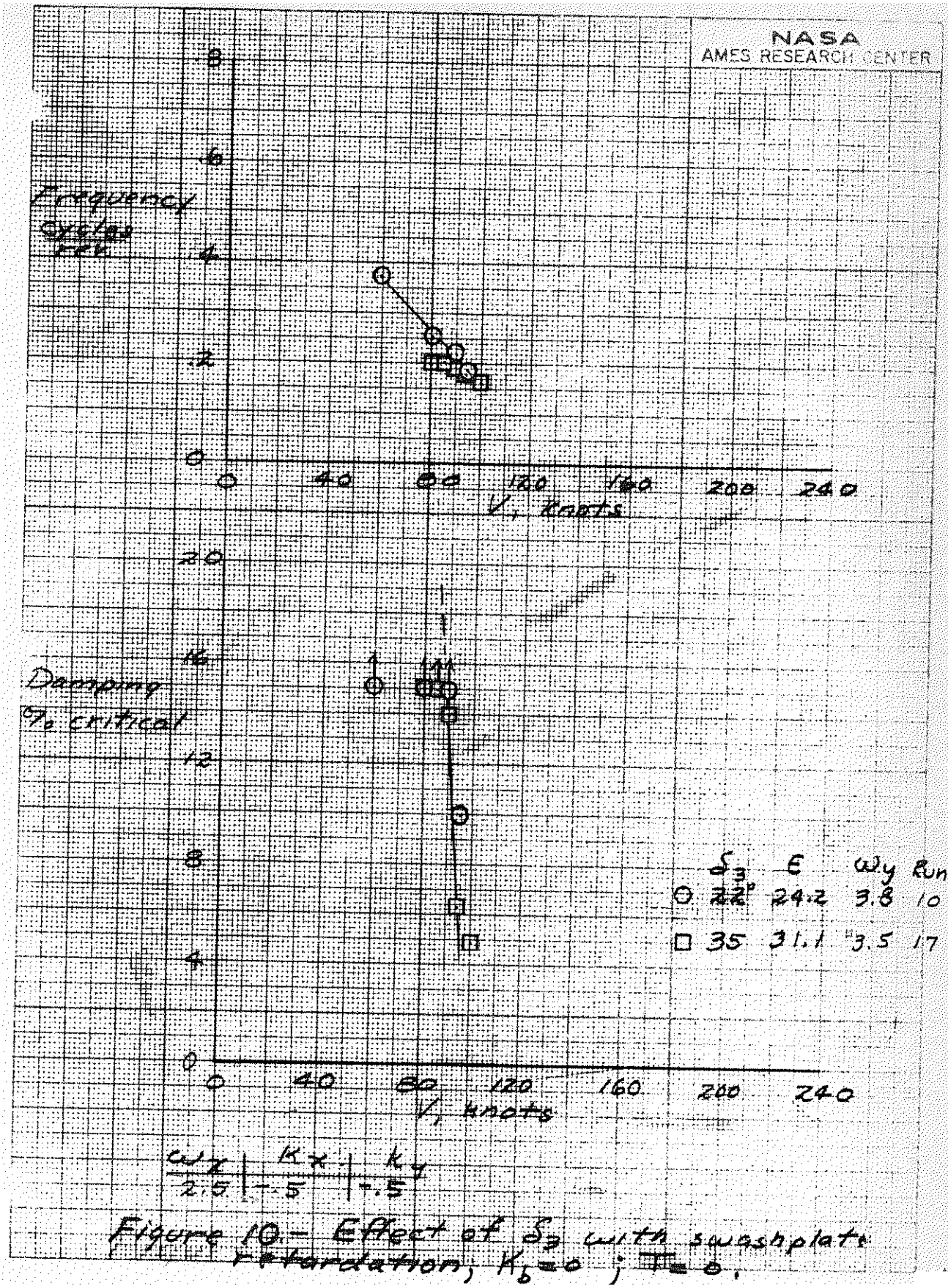

Figure 10.- Effect of δ_3 with squashplate retardation; $K_b = 0$; $\Pi = 0$.

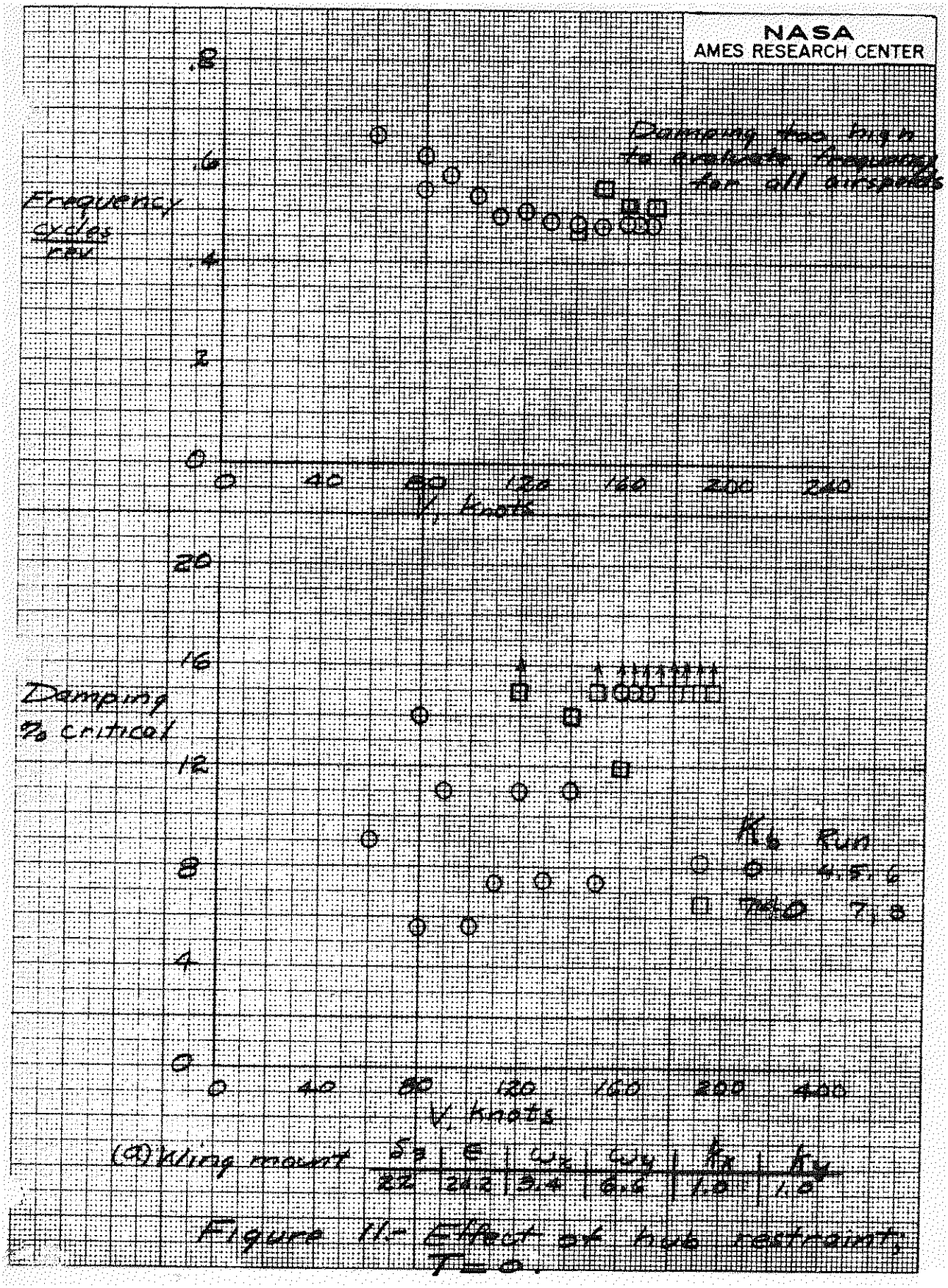

Figure 11.- Effect of hub restraint, $T = 0$.

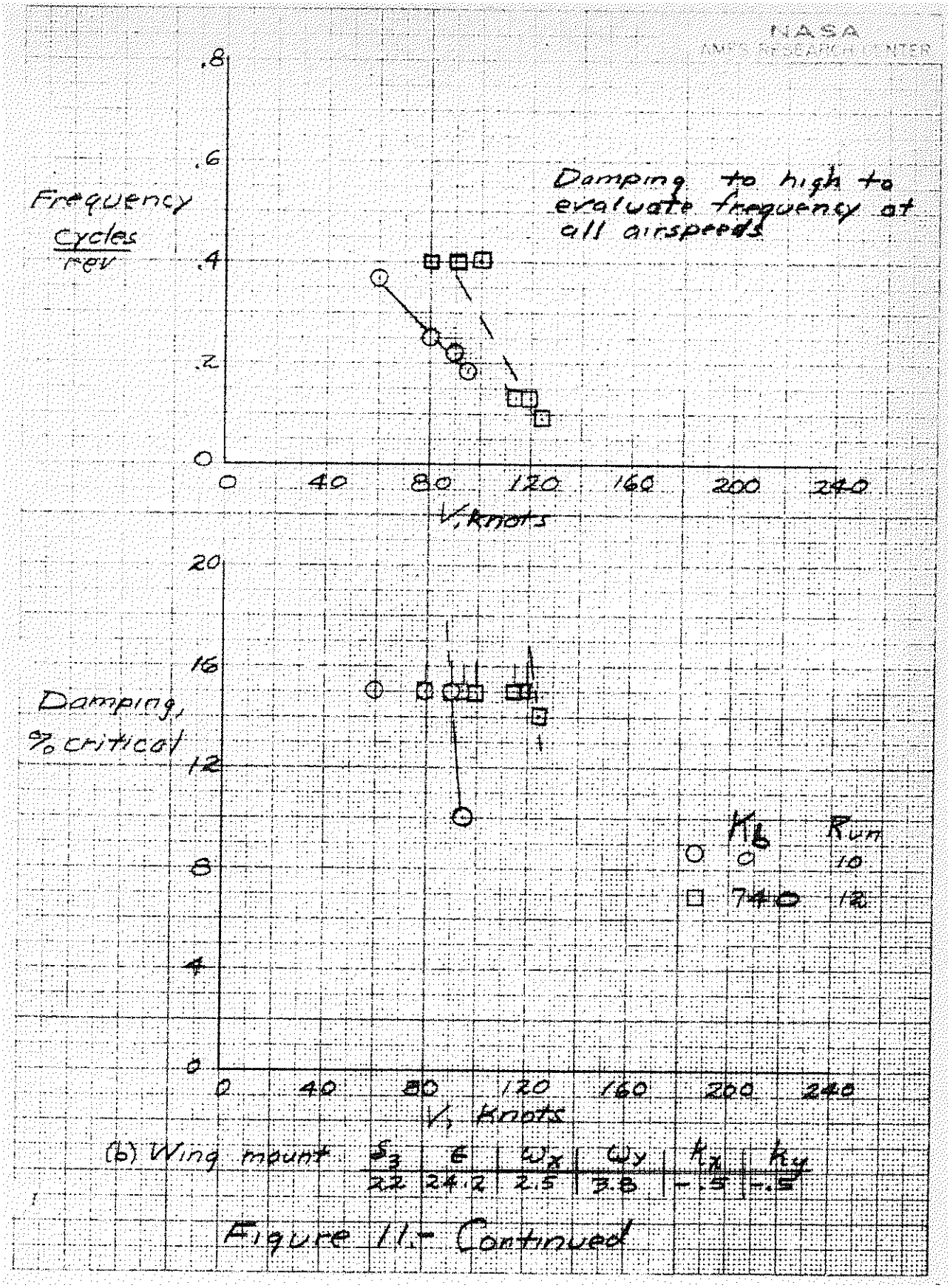

(b) Wing mount

S_3	E	ω_x	ω_y	k_x	k_y
22	24.2	2.5	3.8	-.5	-.5

Figure 11.- Continued

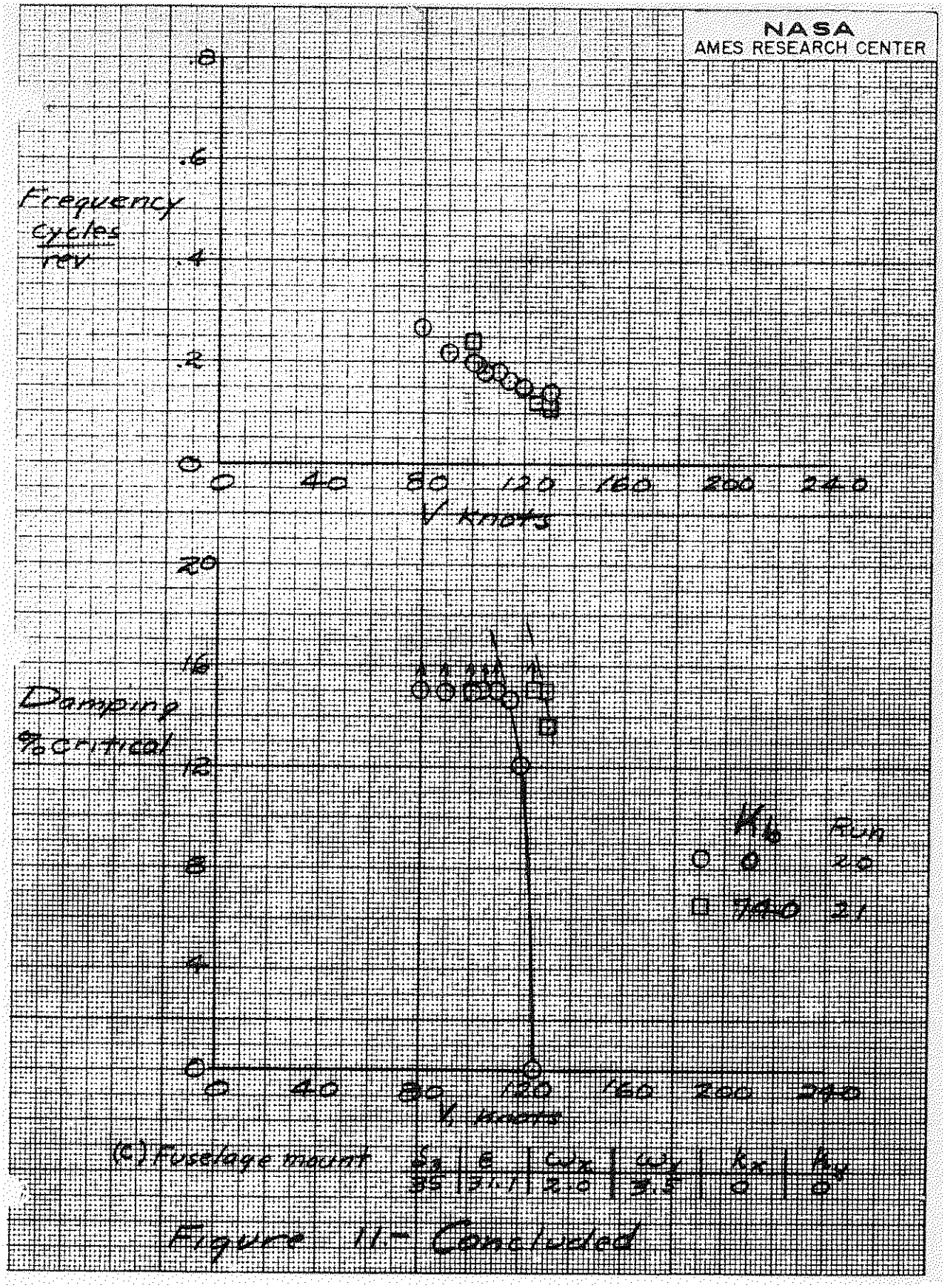

Figure 11.- Concluded

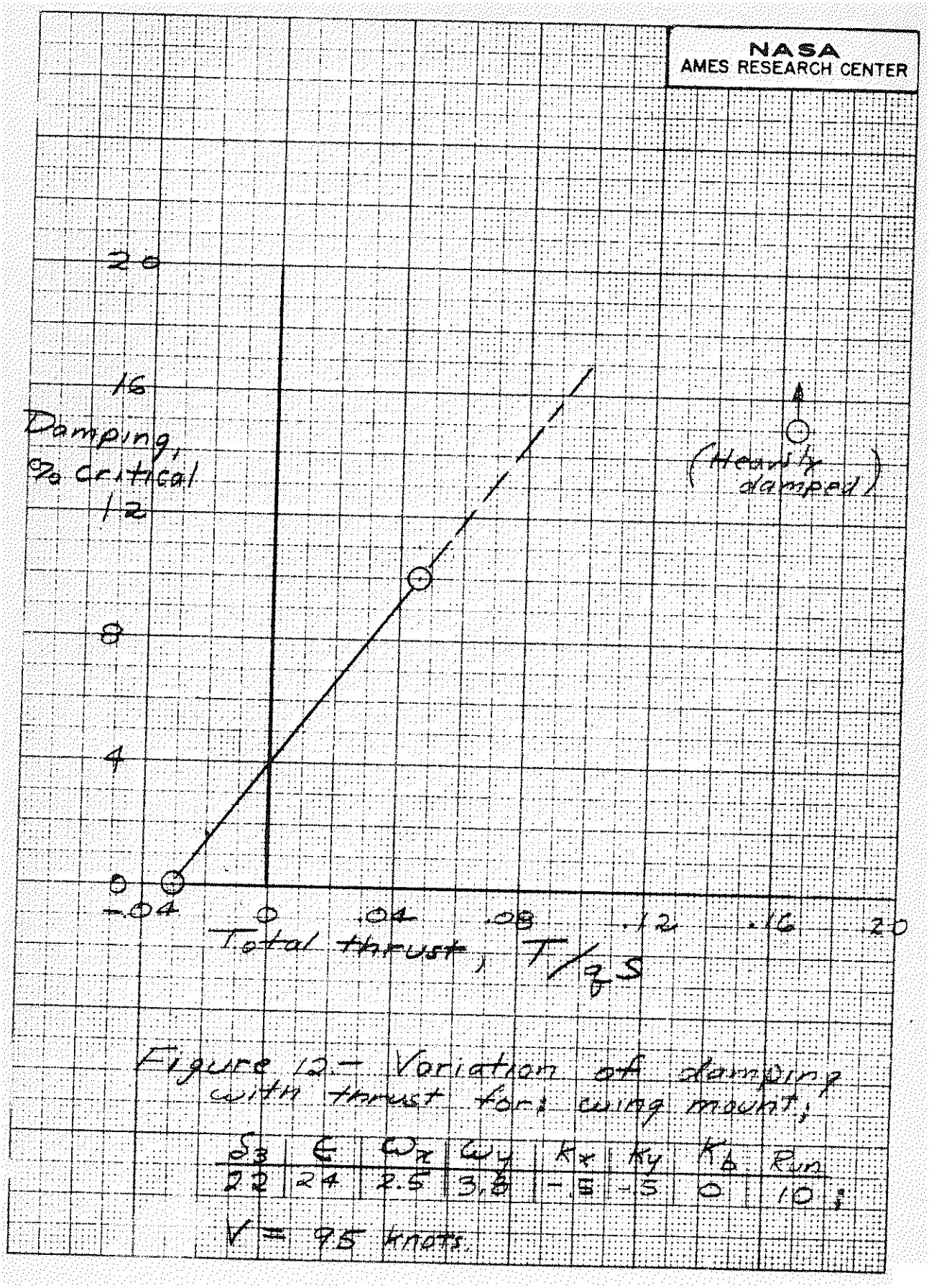

Figure 12.— Variation of damping with thrust for wing mount;

δ_3	ϵ	ω_x	ω_y	k_x	k_y	k_Δ	R_{in}
22	24	2.5	3.8	-.5	-5	0	10

$V = 95$ knots.